Extended Target Fast Labeled Multi-Bernoulli Filter

Xuan CHENG, Hongbing JI, Yongquan ZHANG

School of Electronic Engineering, Xidian University, Xi'an 710071, PR China

chengxuanxd@163.com, hbji@xidian.edu.cn, zhangyq@xidian.edu.cn

Abstract. *Focusing on the real-time tracking of the extended target labeled multi-Bernoulli (ET-LMB) filter, this paper proposes an extended target fast labeled multi-Bernoulli (ET-FLMB) filter based on beta gamma box particle (BGBP) and Gaussian process (GP), called ET-BGBP-GP-FLMB filter. First, a new ET-FLMB filter is derived to reduce the computational complexity of the ET-LMB filter. Then, by modeling the target state as an augmented state including detection probability, measurement rate, kinematic state and extension state, the BGBP-GP implementation of the ET-FLMB filter is presented. Compared with the traditional sequential Monte Carlo (SMC) implementation, the proposed implementation can not only greatly reduce the number of particles and the amount of computation, but also estimate the detection probabilities, measurement rates and extension states while estimating the number and kinematic states of extended targets. Finally, the simulation results show that the proposed filter can significantly reduce the computational burden and improve the real-time performance.*

Keywords

Extended target tracking, fast labeled multi-Bernoulli filter, beta gamma box particle, Gaussian process

1. Introduction

Target tracking plays an extremely important role in both military and civilian fields. According to the number of measurements obtained from a target at each time step, the target can be divided into a point target or an extended target. Point target means that one target can obtain at most one measurement at each time step, while extended target means that one target can obtain multiple measurements at each time step. In this way, target tracking can be divided into point target tracking [1–4] and extended target tracking [5–25]. With the continuous advancement of sensor technology, the sensor resolution is getting higher and higher, resulting in more and more measurement information available for each target. Therefore, extended target tracking algorithms become more and more important.

In recent years, multiple extended target tracking algorithms based on random finite set (RFS) have attracted the attention of many scholars [5–23]. The extended target probability hypothesis density (ET-PHD), extended target cardinalized PHD (ET-CPHD), extended target cardinality balanced multi-target multi-Bernoulli (ET-CBMeMBer), extended target generalized labeled multi-Bernoulli (ET-GLMB), extended target labeled multi-Bernoulli (ET-LMB) and extended target Poisson multi-Bernoulli mixture (ET-PMBM) filters have been proposed in [5–9]. Compared with the early ET-PHD [5], ET-CPHD [6] and ET-CBMeMber [7] filters, the ET-GLMB [8], ET-LMB [8] and ET-PMBM [9] filters have better estimation performance under poor detection conditions. Moreover, the ET-GLMB and ET-LMB filters are based on labeled RFS, and they can output target tracks. The ET-LMB filter is an effective approximation of the ET-GLMB filter, which has less computational burden with slight performance loss. However, the computational complexity of the ET-LMB filter is still high. Therefore, this paper first improves the ET-LMB filter to improve its real-time performance.

The implementation methods of the above filters mainly include Gaussian mixture (GM) implementation [6, 10, 11], sequential Monte Carlo (SMC) implementation [12], [13], gamma Gaussian inverse Wishart (GGIW) implementation [8, 9, 14] and box particle implementation [15–17]. As early implementation methods, GM and SMC implementations can only estimate the number and kinematic states of extended targets [6], [10–13]. The GGIW implementation can not only estimate the number and kinematic states of targets, but also estimate their extension states and measurement rates [8, 9, 14]. However, the GGIW implementation can only estimate the extension states as ellipses. For non-elliptic extension states, some improved algorithms of the above filters are proposed in [18–21]. However, like the GM and GGIW implementations of these filters, most of these improved algorithms are based on the linear Gaussian assumption. For extended target tracking under nonlinear conditions, the SMC or box particle implementations of these filters are required. The SMC implementation often requires a large number of particles, and the computational burden is heavy. Therefore, the box particle implementation is used to reduce the amount of computation. However, the existing filters implemented by SMC or box particles, including the standard PHD and LMB filters implemented by box particles for extended target tracking [22], [23], either do not consider the extension states of targets [15, 22, 23], or only consider the

extension states of simple shapes [16], [17]. As far as we know, there is no report on non-elliptic extension state estimation using RFS filter implemented by box particles. In addition, the existing filters based on box particle and RFS cannot handle the extended target tracking under the condition of unknown detection probability. Therefore, we improve the box particle implementation and propose a method based on beta gamma box particle and Gaussian process (BGBP-GP) to implement the improved ET-LMB filter.

The main contributions of this paper are summarized as follows.

(1) At the filter level, an improved ET-LMB filter, namely the extended target fast LMB (ET-FLMB) filter, is proposed. It combines the prediction step and update step of the ET-LMB filter into one step, and uses Gibbs sampling to select the high weight hypothesis components, effectively reducing the computational complexity of the ET-LMB filter.

(2) At the implementation level, the BGBP-GP implementation of the proposed ET-FLMB filter is given, which is called ET-BGBP-GP-FLMB filter. Compared with the SMC implementation, the box particle implementation can significantly reduce the number of particles and computational burden. In addition, the detection probability, measurement rate and extension state are modeled as beta distribution, gamma distribution and Gaussian process [24] respectively. The proposed implementation can not only estimate the number and kinematic states of extended targets, but also estimate their detection probabilities, measurement rates and extension states.

(3) A likelihood function that considers the detection probability, measurement rate and kinematic state is proposed to form the closed recurrence of the ET-FLMB filter. What's more, a separate extension state likelihood function is also presented, which enables the proposed filter to estimate extension states with arbitrary star-convex shapes.

(4) In terms of performance evaluation, the OSPA distance variants of the extension states and detection probabilities of multiple extended targets are given.

The remainder of the paper is organized as follows. Section 2 mainly introduces the extended target state models, measurement model and GP principle. The main steps of the proposed ET-FLMB filter are presented in Sec. 3. In Sec. 4, the specific form of measurement likelihood function is given, and the BGBP-GP implementation of the ET-FLMB filter is presented. Then, the performance evaluation criteria are introduced, and the advantages of the proposed filter are discussed. The simulations and analyses are given in Sec. 5. The last section presents the conclusions and future work.

2. Extended Target Models

In this section, we mainly introduce the extended target state models, measurement model and GP principle. For readability, some notations are first introduced in Sec. 2.1.

2.1 Some Notations

(1) The generalized Kronecker delta function and generalized inclusion function are respectively defined as $\delta_Y(X) \triangleq \begin{cases} 1, & \text{if } X = Y \\ 0, & \text{otherwise} \end{cases}$ and $1_Y(X) \triangleq \begin{cases} 1, & \text{if } X \subseteq Y \\ 0, & \text{otherwise} \end{cases}$, where X and Y are unlabeled state sets.

(2) The multi-target exponential function is defined as $[h(\cdot)]^X \triangleq \prod_{\mathbf{x} \in X} h(\mathbf{x})$, where $h(\mathbf{x})$ is a real valued function and $h^\varnothing = 1$.

(3) The label indicator function is defined as $\triangle(\mathbf{X}) \triangleq \begin{cases} 1, & \text{if } |\mathcal{L}(\mathbf{X})| = |\mathbf{X}| \\ 0, & \text{if } |\mathcal{L}(\mathbf{X})| \neq |\mathbf{X}| \end{cases}$, where $\mathbf{X}$ is a labeled state set, $\mathcal{L}(\mathbf{X})$ is the set of unique labels in this set, and $|\mathbf{X}|$ is the number of elements in $\mathbf{X}$.

(4) $\beta(D; s, t) = D^{s-1}(1 - D)^{t-1} / B(s, t)$ is the beta probability density function, where $D \in [0,1]$, $s > 0$, $t > 0$, $B(s, t) = \Gamma(s)\Gamma(t)/\Gamma(s + t)$, and $\Gamma(\cdot)$ is the gamma function.

(5) $\mathcal{GAM}(\gamma; \alpha, \beta) = (\beta^\alpha / \Gamma(\alpha))\gamma^{\alpha-1} e^{-\beta\gamma}$ is the gamma probability density function, where $\gamma > 0$, $\alpha > 0$, $\beta > 0$.

2.2 Extended Target State Models

In this work, the state set of extended targets at time k is expressed as follows

$$\mathbf{X}_k = \{(\xi_k^{(i)}, \mathbf{l}_k^{(i)})\}_{i=1}^{|\mathbf{X}_k|}, \quad \xi_k^{(i)} \triangleq (D_k^{(i)}, \gamma_k^{(i)}, \mathbf{x}_k^{K,(i)}, \mathbf{x}_k^{E,(i)}) \quad (1)$$

where $\mathbf{X}_k$ is the state set of extended targets, $|\mathbf{X}_k|$ the number of extended targets in this set, $\xi_k^{(i)}$ the state of the ith extended target, $\mathbf{l}_k^{(i)}$ the target label, $D_k^{(i)}$ the detection probability, $\gamma_k^{(i)}$ the measurement rate, $\mathbf{x}_k^{K,(i)}$ the kinematic state, and $\mathbf{x}_k^{E,(i)}$ the extension state. The evolution models of detection probability, measurement rate, kinematic state and extension state of each extended target are as follows.

(1) Detection probability: It is modeled as a beta distribution, and the prediction parameters are as follows

$$s_{k|k-1}^{(i)} = (\mu_{D,k|k-1}^{(i)}(1-\mu_{D,k|k-1}^{(i)})/(\sigma_{D,k|k-1}^{(i)})^2 - 1)\mu_{D,k|k-1}^{(i)}, \quad (2)$$

$$t_{k|k-1}^{(i)} = (\mu_{D,k|k-1}^{(i)}(1-\mu_{D,k|k-1}^{(i)})/(\sigma_{D,k|k-1}^{(i)})^2 - 1)(1-\mu_{D,k|k-1}^{(i)}), \quad (3)$$

$$\mu_{D,k|k-1}^{(i)} = \mu_{D,k-1}^{(i)} = s_{k-1}^{(i)}/(s_{k-1}^{(i)}+t_{k-1}^{(i)}), \quad (4)$$

$$(\sigma_{D,k|k-1}^{(i)})^2 = \upsilon_D(\sigma_{D,k-1}^{(i)})^2 = \upsilon_D \frac{s_{k-1}^{(i)}t_{k-1}^{(i)}}{(s_{k-1}^{(i)}+t_{k-1}^{(i)})^2(s_{k-1}^{(i)}+t_{k-1}^{(i)}+1)} \quad (5)$$

where $\mu_{D,k|k-1}^{(i)}$ and $(\sigma_{D,k|k-1}^{(i)})^2$ are the predicted mean and variance, respectively. In general, we choose $\upsilon_D > 1$, which means that the mean of detection probability does not change, and the variance becomes larger. In addition, for consistency reasons, the choice of parameters must satisfy condition $(\sigma_{D,k|k-1}^{(i)})^2 < \mu_{D,k|k-1}^{(i)}(1-\mu_{D,k|k-1}^{(i)})$.

(2) Measurement rate: It is modeled as a gamma distribution, and the predicted parameters are as follows

$$\alpha_{k|k-1}^{(i)} = \alpha_{k-1}^{(i)}/\eta_\gamma, \quad \beta_{k|k-1}^{(i)} = \beta_{k-1}^{(i)}/\eta_\gamma \quad (6)$$

where $\eta_\gamma > 1$ is an exponential forgetting factor.

(3) Kinematic state: Under the framework of interval analysis, its prediction process is expressed as follows

$$[\mathbf{x}_k^{K,(i)}] = [f_{\mathbf{x}^K,k|k-1}]([\mathbf{x}_{k-1}^{K,(i)}]) + [\mathbf{w}_k^{K,(i)}] \quad (7)$$

where $[\mathbf{x}_k^{K,(i)}]$ is the kinematic state with interval form, $[f_{\mathbf{x}^K,k|k-1}]$ the transfer function, and $[\mathbf{w}_k^{K,(i)}]$ the process noise.

(4) Extension state: It is described by a star-convex shape [24]. Thus, it can be denoted by a vector composed of radial function values. In this work, we sample N^E points in interval $[0,2\pi]$ at equal intervals, i.e. $\boldsymbol{\theta}^E = (\theta_1^E, \cdots, \theta_{N^E}^E)^T$. Then, the extension state can be denoted by their corresponding radial function values, i.e. $\mathbf{x}^E = (r_1^E, \cdots, r_{N^E}^E)^T = (f^E(\theta_1^E), \cdots, f^E(\theta_{N^E}^E))^T$. The star-convex shape and corresponding radial function are shown in Fig. 1.

In Fig. 1(a), a star-convex shape is shown in the global coordinate system. The measurements and target kinematic state are described in this coordinate system. The radial function is described in the local coordinate system. The origin of local coordinate system is the position of target centroid. The radial function corresponding to the star-convex shape is shown in Fig. 1(b).

The transition process of extension state is as follows

$$\mathbf{x}_k^{E,(i)} = \mathbf{F}^E \mathbf{x}_{k-1}^{E,(i)} + \mathbf{w}_k^{E,(i)}, \quad \mathbf{w}_k^{E,(i)} \sim \mathcal{N}(\mathbf{0}, \mathbf{Q}^E), \quad (8)$$

$$\mathbf{F}^E = e^{-\alpha^E T}\mathbf{I}, \quad \mathbf{Q}^E = (1-e^{-2\alpha^E T})\mathbf{C}^E(\boldsymbol{\theta}^E, \boldsymbol{\theta}^E), \quad (9)$$

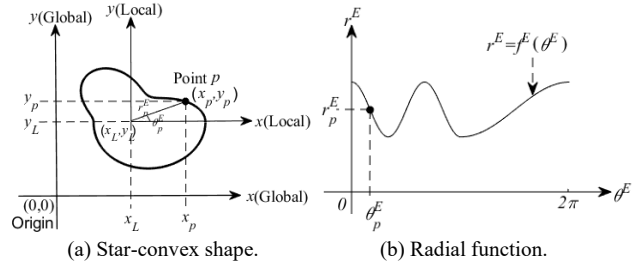(a) Star-convex shape.   (b) Radial function.

Fig. 1. The star-convex shape and corresponding radial function.

$$\mathbf{C}^E(\boldsymbol{\theta}^E, \boldsymbol{\theta}^E) = \begin{bmatrix} c^E(\theta_1^E, \theta_1^E) & \cdots & c^E(\theta_1^E, \theta_{N^E}^E) \\ \vdots & & \vdots \\ c^E(\theta_{N^E}^E, \theta_1^E) & \cdots & c^E(\theta_{N^E}^E, \theta_{N^E}^E) \end{bmatrix} \quad (10)$$

where $\mathbf{F}^E$ is the extension state transition matrix, and $\mathbf{w}_k^{E,(i)}$ the extension state process noise. α^E can be regarded as a forgetting factor, and a larger α^E means that less weight is given to older measurements. T is the sampling interval, $\mathbf{I}$ the identity matrix, and $\mathbf{C}^E(\boldsymbol{\theta}^E, \boldsymbol{\theta}^E)$ an N^E dimensional covariance matrix. The covariance function is designed as

$$c^E(\theta_m^E, \theta_n^E) = \sigma_f^2 \, e^{-(2\sin^2(|\theta_m^E-\theta_n^E|/2)/l^2)} + \sigma_r^2 \quad (11)$$

where θ_m^E and θ_n^E are any two angles in interval $[0,2\pi]$, σ_f is the priori standard deviation of signal amplitude, l is the length scale of radial function, and σ_r is the contribution from the unknown mean function.

2.3 Extended Target Measurement Model

In this paper, it is assumed that the measurements generated by each extended target originate from the target contour. Thus, the measurement equation can be written as

$$\mathbf{z}_{k,j}^{(i)} = \mathbf{x}_k^{c,(i)} + \mathbf{p}_k^{E,(i)}(\theta_{k,j}^{E,(i)})f_k^{E,(i)}(\theta_{k,j}^{E,(i)}) + \mathbf{v}_{k,j}^{(i)}, \quad (12)$$

$$\mathbf{p}_k^{E,(i)}(\theta_{k,j}^{E,(i)}) = (\cos(\theta_{k,j}^{E,(i)}), \sin(\theta_{k,j}^{E,(i)}))^T \quad (13)$$

where $\mathbf{x}_k^{c,(i)} = (\mathbf{x}_{x,k}^{K,(i)}, \mathbf{x}_{y,k}^{K,(i)})^T$ is the position of the ith extended target at time k, $\{\mathbf{z}_{k,j}^{(i)}\}_{j=1}^{N_{z,k}^{(i)}}$ are the $N_{z,k}^{(i)}$ measurements generated by this extended target, $\theta_{k,j}^{E,(i)}$ is the angle of measurement $\mathbf{z}_{k,j}^{(i)}$ in the local coordinate system, $\mathbf{v}_{k,j}^{(i)}$ is a zero mean Gaussian measurement noise with covariance $\mathbf{R}$, and $(\cdot)^T$ denotes the transpose operation. Note that the radial function is modeled as a GP. Therefore, the GP principle is introduced in the following.

2.4 GP Principle

Typically, the GP is used to learn an unknown function from the training data. Consider the following measurement model

$$z_{k,j}^{\mathrm{E}} = f_k^{\mathrm{E}}(\theta_{k,j}^{\mathrm{E}}) + v_{k,j}^{\mathrm{E}}, \ v_{k,j}^{\mathrm{E}} \sim \mathcal{N}(0, R^{\mathrm{E}}) \qquad (14)$$

where $z_{k,j}^{\mathrm{E}}$ is the measurement corresponding to the training input $\theta_{k,j}^{\mathrm{E}}$, and it is formed by adding a Gaussian noise $v_{k,j}^{\mathrm{E}}$ to a radial function value $f_k^{\mathrm{E}}(\theta_{k,j}^{\mathrm{E}})$. Our goal is to learn the function value $\mathbf{f}_k^{\mathrm{E}} \triangleq (f_k^{\mathrm{E}}(\theta_{k,1}^{\mathrm{E}}), \cdots, f_k^{\mathrm{E}}(\theta_{k,N^{\mathrm{E}}}^{\mathrm{E}}))^{\mathrm{T}}$ corresponding to the given test input $\boldsymbol{\theta}_k^{\mathrm{E}} \triangleq (\theta_{k,1}^{\mathrm{E}}, \cdots, \theta_{k,N^{\mathrm{E}}}^{\mathrm{E}})^{\mathrm{T}}$ by the given measurement set $\mathbf{z}_k^{\mathrm{E}} \triangleq (z_{k,1}^{\mathrm{E}}, \cdots, z_{k,N_z}^{\mathrm{E}})^{\mathrm{T}}$ and its corresponding input $\dot{\boldsymbol{\theta}}_k^{\mathrm{E}} \triangleq (\dot{\theta}_{k,1}^{\mathrm{E}}, \cdots, \dot{\theta}_{k,N_z}^{\mathrm{E}})^{\mathrm{T}}$.

According to [24], the measurement $z_{k,j}^{\mathrm{E}}$ and the function value f_k^{E} are jointly Gaussian,

$$\begin{pmatrix} z_{k,j}^{\mathrm{E}} \\ \mathbf{f}_k^{\mathrm{E}} \end{pmatrix} \sim \mathcal{N}\left(0, \begin{bmatrix} c^{\mathrm{E}}(\dot{\theta}_{k,j}^{\mathrm{E}}, \dot{\theta}_{k,j}^{\mathrm{E}}) + R^{\mathrm{E}} & \mathbf{C}^{\mathrm{E}}(\dot{\theta}_{k,j}^{\mathrm{E}}, \boldsymbol{\theta}_k^{\mathrm{E}}) \\ \mathbf{C}^{\mathrm{E}}(\boldsymbol{\theta}_k^{\mathrm{E}}, \dot{\theta}_{k,j}^{\mathrm{E}}) & \mathbf{C}^{\mathrm{E}}(\boldsymbol{\theta}_k^{\mathrm{E}}, \boldsymbol{\theta}_k^{\mathrm{E}}) \end{bmatrix} \right). (15)$$

Thus, the extension state likelihood can be written as

$$g^{\mathrm{E}}(z_{k,j}^{\mathrm{E}} \mid \mathbf{f}_k^{\mathrm{E}}) = \mathcal{N}(z_{k,j}^{\mathrm{E}}; \mathbf{H}_k^{\mathrm{E}} \mathbf{f}_k^{\mathrm{E}}, R_k^{g^{\mathrm{E}}}), \qquad (16)$$

$$\mathbf{H}_k^{\mathrm{E}}(\dot{\theta}_{k,j}^{\mathrm{E}}) = \mathbf{C}^{\mathrm{E}}(\dot{\theta}_{k,j}^{\mathrm{E}}, \boldsymbol{\theta}_k^{\mathrm{E}})(\mathbf{C}^{\mathrm{E}}(\boldsymbol{\theta}_k^{\mathrm{E}}, \boldsymbol{\theta}_k^{\mathrm{E}}))^{-1}, \qquad (17)$$

$$R_k^{g^{\mathrm{E}}}(\dot{\theta}_{k,j}^{\mathrm{E}}) = c^{\mathrm{E}}(\dot{\theta}_{k,j}^{\mathrm{E}}, \dot{\theta}_{k,j}^{\mathrm{E}}) + R^{\mathrm{E}} - \\ \mathbf{C}^{E}(\dot{\theta}_{k,j}^{\mathrm{E}}, \boldsymbol{\theta}_k^{\mathrm{E}})(\mathbf{C}^{\mathrm{E}}(\boldsymbol{\theta}_k^{\mathrm{E}}, \boldsymbol{\theta}_k^{\mathrm{E}}))^{-1} \mathbf{C}^{\mathrm{E}}(\boldsymbol{\theta}_k^{\mathrm{E}}, \dot{\theta}_{k,j}^{\mathrm{E}}). \quad (18)$$

Further, according to (16) and [24], the measurement Equation (12) can finally be written as

$$\mathbf{z}_{k,j}^{(i)} = h_{k,j}^{(i)}(\mathbf{x}_k^{c,(i)}, \mathbf{f}_k^{\mathrm{E},(i)}) + \overline{\mathbf{v}}_{k,j}^{(i)}, \ \overline{\mathbf{v}}_{k,j}^{(i)} \sim \mathcal{N}(0, \overline{\mathbf{R}}_{k,j}^{(i)}), \quad (19)$$

$$h_{k,j}^{(i)}(\mathbf{x}_k^{c,(i)}, \mathbf{f}_k^{\mathrm{E},(i)}) = \mathbf{x}_k^{c,(i)} + \mathbf{p}_k^{\mathrm{E},(i)}(\theta_{k,j}^{\mathrm{E}}) \mathbf{H}_k^{\mathrm{E},(i)}(\theta_{k,j}^{\mathrm{E}}) \mathbf{f}_k^{\mathrm{E},(i)}, \quad (20)$$

$$\overline{\mathbf{R}}_{k,j}^{(i)} = \mathbf{p}_k^{\mathrm{E},(i)}(\theta_{k,j}^{\mathrm{E},(i)}) R_k^{g^{\mathrm{E}}}(\dot{\theta}_{k,j}^{\mathrm{E}})(\mathbf{p}_k^{\mathrm{E},(i)}(\theta_{k,j}^{\mathrm{E},(i)}))^{\mathrm{T}} + \mathbf{R}. \quad (21)$$

Considering that the measurement noise is already included in (21), the R^{E} in (18) can be omitted.

3. ET-FLMB Filter

In this section, the measurement likelihood function is first introduced. And then, the main steps of the ET-FLMB filter are presented, which fuses the prediction and update into one step and uses Gibbs sampling to calculate the hypothesis components with larger weights.

3.1 Measurement Likelihood Function

The measurement likelihood function used in this paper is similar to the ET-LMB filter [8]. It is given as

$$g(Z_k \mid \mathbf{X}_k) = g_C(Z_k) \sum_{i=1}^{|\mathbf{X}_k|+1} \sum_{\substack{\mathcal{U}(Z_k) \in \mathcal{P}_i(Z_k) \\ \theta \in \Theta(\mathcal{U}(Z_k))}} [\psi_{\mathcal{U}(Z_k)}(\cdot; \theta)]^{\mathbf{X}_k}, (22)$$

$$\psi_{\mathcal{U}(Z_k)}(\xi_k, \mathbf{l}_k; \theta) = \psi_{\mathcal{U}(Z_k)}(D_k, \gamma_k, \mathbf{x}_k^{\mathrm{K}}, \mathbf{x}_k^{\mathrm{E}}, \mathbf{l}_k; \theta)$$

$$= \begin{cases} \dfrac{D_k(\mathbf{l}_k) \tilde{g}(\mathcal{U}_{\theta(\mathbf{l}_k)}(Z_k) \mid \gamma_k, \mathbf{x}_k^{\mathrm{K}}, \mathbf{x}_k^{\mathrm{E}}, \mathbf{l}_k)}{[\kappa]^{\mathcal{U}_{\theta(\mathbf{l}_k)}(Z_k)}}, & \theta(\mathbf{l}_k) > 0 \\ 1 - D_k(\mathbf{l}_k), & \theta(\mathbf{l}_k) = 0 \end{cases} (23)$$

where $g_C(K) = \mathrm{e}^{-\langle \kappa, 1 \rangle} \kappa^K$, κ is the intensity function of clutter Poisson RFS K. $\mathcal{P}_i(Z_k)$ is the set of measurement partitions that just divide the measurement set Z_k into i groups, $\mathcal{U}(Z_k) \in \mathcal{P}_i(Z_k)$ is a particular partition of $\mathcal{P}_i(Z_k)$. $\Theta(\mathcal{U}(Z_k))$ is the space of association mappings $\theta : \mathcal{L}(\mathbf{X}_k) \rightarrow \{0, 1, \cdots, |\mathcal{U}(Z_k)|\}$, where $\theta(\mathbf{l}_k) = \theta(\mathbf{l}_k') > 0$ means $\mathbf{l}_k = \mathbf{l}_k'$. $\tilde{g}(\mathcal{U}_{\theta(\mathbf{l}_k)}(Z_k) \mid \gamma_k, \mathbf{x}_k^{\mathrm{K}}, \mathbf{x}_k^{\mathrm{E}}, \mathbf{l}_k)$ is the likelihood function for a single measurement partition cell $\mathcal{U}_{\theta(\mathbf{l}_k)}(Z_k)$.

3.2 The Main Steps of the ET-FLMB Filter

(1) *Joint prediction and update:* Suppose that the multiple extended target posterior density at time $k-1$ can be denoted by an LMB RFS [8] with parameter set $\boldsymbol{\pi}_{k-1} = \{(r_{k-1}^{(\mathbf{l}_{k-1})}, p_{k-1}^{(\mathbf{l}_{k-1})})\}_{\mathbf{l}_{k-1} \in \mathbb{L}_{k-1}}$, where $r_{k-1}^{(\mathbf{l}_{k-1})}$ and $p_{k-1}^{(\mathbf{l}_{k-1})}$ denote the existence probability and probability density of target $\mathbf{l}_{k-1}$ respectively, and $\mathbb{L}_{k-1}$ denotes the label space at time $k-1$. At the same time, suppose that the newborn multiple extended target density at time k can be denoted by an LMB RFS with parameter set $\boldsymbol{\pi}_{B,k} = \{(r_{B,k}^{(\mathbf{l}_k)}, p_{B,k}^{(\mathbf{l}_k)})\}_{\mathbf{l}_k \in \mathbb{B}_k}$, where $r_{B,k}^{(\mathbf{l}_k)}$ and $p_{B,k}^{(\mathbf{l}_k)}$ denote existence probability and probability density of newborn target respectively, and $\mathbb{B}_k$ denotes the label space of the newborn target at time k. Then, the multiple extended target posterior density after joint prediction and update at time k can be written as

$$\boldsymbol{\pi}_k(\mathbf{X}_k \mid Z_k) = \Delta(\mathbf{X}_k) \cdot$$

$$\sum_{I_k \in \mathcal{F}(\mathbb{L}_k)} \sum_{i=1}^{|\mathbf{X}_k|+1} \sum_{\substack{\mathcal{U}(Z_k) \in \mathcal{P}_i(Z_k) \\ \theta \in \Theta(\mathcal{U}(Z_k))}} w_{\mathcal{U}(Z_k)}^{(I_k, \theta)} \delta_{I_k}(\mathcal{L}(\mathbf{X}_k)) [p_k^{(\theta)}(\cdot \mid \mathcal{U}(Z_k))]^{\mathbf{X}_k}, (24)$$

$$w_{\mathcal{U}(Z_k)}^{(I_k, \theta)} \propto 1_{\Theta(I_k)}(\theta)[1 - r_{k-1} \eta_{S,k|k-1}]^{\mathbb{L}_{k-1} - I_k} \cdot$$

$$[r_{k-1} \eta_{S,k|k-1}]^{\mathbb{L}_{k-1} \cap I_k} [1 - r_{B,k}]^{\mathbb{B}_k - I_k} [r_{B,k}]^{\mathbb{B}_k \cap I_k} [\overline{\psi}_{\mathcal{U}(Z_k)}^{(\theta)}]^{I_k}, (25)$$

$$\eta_{S,k|k-1}(\mathbf{l}_k) = \iint p_{S,k}(\xi_{k-1}, \mathbf{l}_{k-1}) \cdot$$

$$f_{k|k-1}(\xi_k \mid \xi_{k-1}, \mathbf{l}_k) p_{k-1}^{(\mathbf{l}_{k-1})}(\xi_{k-1}) \, \mathrm{d}\xi_{k-1} \, \mathrm{d}\xi_k, \quad (26)$$

$$\overline{\psi}_{\mathcal{U}(Z_k)}^{(\theta)}(\mathbf{l}_k) = \int p_{k|k-1}^{(\mathbf{l}_k)}(\xi_k) \psi_{\mathcal{U}(Z_k)}(\xi_k, \mathbf{l}_k; \theta) \, \mathrm{d}\xi_k, \quad (27)$$

$$p_{k|k-1}^{(\mathbf{l}_k)}(\xi_k) = 1_{\mathbb{L}_{k-1}}(\mathbf{l}_k) \cdot$$

$$\dfrac{\int p_{S,k}(\xi_{k-1}, \mathbf{l}_{k-1}) f_{k|k-1}(\xi_k \mid \xi_{k-1}, \mathbf{l}_k) p_{k-1}^{(\mathbf{l}_{k-1})}(\xi_{k-1}) \, \mathrm{d}\xi_{k-1}}{\eta_{S,k|k-1}(\mathbf{l}_k)} \quad (28)$$

$$+ 1_{\mathbb{B}_k}(\mathbf{l}_k) p_{B,k}^{(\mathbf{l}_k)}(\xi_k),$$

$$p_k^{(\theta)}(\xi_k, \mathbf{l}_k \mid \mathcal{U}(Z_k)) = \frac{p_{k|k-1}^{(\mathbf{l}_k)}(\xi_k)\psi_{\mathcal{U}(Z_k)}(\xi_k, \mathbf{l}_k; \theta)}{\overline{\psi}_{\mathcal{U}(Z_k)}^{(\theta)}(\mathbf{l}_k)} \quad (29)$$

where $\mathbb{L}_k = \mathbb{B}_k \bigcup \mathbb{L}_{k-1}(\mathbb{L}_{k-1} \bigcap \mathbb{B}_k = \varnothing)$ is the label space at time k, $w_{\mathcal{U}(Z_k)}^{(\mathbf{l}_k, \theta)}$ the weight of different GLMB components, $p_{k|k-1}^{(\mathbf{l}_k)}(\xi_k)$ the single target prediction density, $p_{S,k}(\xi_{k-1}, \mathbf{l}_{k-1})$ the survival probability, $f_{k|k-1}(\xi_k \mid \xi_{k-1}, \mathbf{l}_k)$ the state transition function, and $p_k^{(\theta)}(\xi_k, \mathbf{l}_k \mid \mathcal{U}(Z_k))$ the single target posterior density. Equation (24) is actually a GLMB density [8], and it needs to be approximated as an LMB to form a closed recurrence. By first-order moment matching, this GLMB density can be approximated as an LMB RFS with parameter set $\boldsymbol{\pi}_k = \{(r_k^{(\mathbf{l}_k)}, p_k^{(\mathbf{l}_k)})\}_{\mathbf{l}_k \in \mathbb{L}_k}$, where

$$r_k^{(\mathbf{l}_k)} = \sum_{I_k \in \mathcal{F}(\mathbb{L}_k)} \sum_{i=1}^{|I_k|+1} \sum_{\substack{\mathcal{U}(Z_k) \in \mathcal{P}_i(Z_k) \\ \theta \in \Theta(\mathcal{U}(Z_k))}} w_{\mathcal{U}(Z_k)}^{(I_k, \theta)} 1_{I_k}(\mathbf{l}_k), \quad (30)$$

$$p_k^{(\mathbf{l}_k)}(\xi_k) = 1/r_k^{(\mathbf{l}_k)} \cdot$$
$$\sum_{I_k \in \mathcal{F}(\mathbb{L}_k)} \sum_{i=1}^{|I_k|+1} \sum_{\substack{\mathcal{U}(Z_k) \in \mathcal{P}_i(Z_k) \\ \theta \in \Theta(\mathcal{U}(Z_k))}} w_{\mathcal{U}(Z_k)}^{(I_k, \theta)} 1_{I_k}(\mathbf{l}_k) p_k^{(\theta)}(\xi_k, \mathbf{l}_k \mid \mathcal{U}(Z_k)). \quad (31)$$

(2) *Cost matrix and Gibbs sampling:* In the above joint prediction and update, in order to compute the hypothesis components with larger weights, an extended cost matrix needs to be calculated, which comprehensively considers survival, death, birth, detection and missed detection.

Here, we consider a fixed $\mathcal{U}(Z_k) = \{W_{1:M}\}$, $I_{k-1} = \{\mathbf{l}_{1:R}\}$, and $\mathbb{B}_k = \{\mathbf{l}_{R+1:P}\}$, where W is a measurement partition cell in $\mathcal{U}(Z_k)$. Our goal is to search for a set of pairs $(I_k, \theta) \in \mathcal{F}(\mathbb{L}_k) \times \Theta(I_k)$ with significant weight $w_{\mathcal{U}(Z_k)}^{(I_k, \theta)}$. For each pair (I_k, θ), $\gamma = (\gamma_{1:P}) \in \{-1:M\}^P$ is defined by

$$\gamma_i = \begin{cases} \theta(\mathbf{l}_i), \text{if } \mathbf{l}_i \in I_k \\ -1, \text{ otherwise.} \end{cases} \quad (32)$$

Considering that γ inherits the positive 1-1 property of θ, there is no difference $i, i' \in \{1:P\}$ with $\gamma_i = \gamma_{i'} > 0$. We use $\dot{\Gamma}$ to denote the set of all positive 1-1 elements of $\{-1:M\}^P$. Thus, there is $\gamma \in \dot{\Gamma}$, and we can recover the labels I_k and associations $\theta : I_k \to \{0:M\}$ by $I_k = \{\mathbf{l}_i \in I_{k-1} \bigcup \mathbb{B}_k : \gamma_i \geq 0\}$ and $\theta(\mathbf{l}_i) = \gamma_i$, respectively.

For all $i \in \{1:P\}$, we define

$$\eta_i(j) = \begin{cases} 1 - \eta_{S,k|k-1}(\mathbf{l}_i)r_{k-1}^{(\mathbf{l}_i)}, & 1 \leq i \leq R, j < 0 \\ \eta_{S,k|k-1}(\mathbf{l}_i)r_{k-1}^{(\mathbf{l}_i)}\overline{\psi}_{\mathcal{U}(Z_k)}^{(j)}(\mathbf{l}_i), & 1 \leq i \leq R, j \geq 0 \\ 1 - r_{B,k}(\mathbf{l}_i), & R+1 \leq i \leq P, j < 0 \\ r_{B,k}(\mathbf{l}_i)\overline{\psi}_{\mathcal{U}(Z_k)}^{(j)}(\mathbf{l}_i), & R+1 \leq i \leq P, j \geq 0 \end{cases} \quad (33)$$

where $1 \leq i \leq R$ corresponds to the surviving targets and $R+1 \leq i \leq P$ the newborn targets. $j \in \{-1:M\}$ denotes the index of the cell W assigned to track $\mathbf{l}_i$, where $j = -1$ denotes the death of track $\mathbf{l}_i$, and $j = 0$ the missed detection of track $\mathbf{l}_i$. Further, (25) can be written as $w_{\mathcal{U}(Z_k)}^{(I_k, \theta)} \propto 1_{\dot{\Gamma}}(\gamma)\prod_{i=1}^P \eta_i(\gamma_i)$, where $1_{\dot{\Gamma}}(\gamma) = 1_{\Theta(I_k)}(\theta)$. Thus, searching the set of pairs $(I_k, \theta) \in \mathcal{F}(\mathbb{L}_k) \times \Theta(I_k)$ with significant weight $w_{\mathcal{U}(Z_k)}^{(I_k, \theta)}$ is equivalent to searching the set of positive 1-1 vectors γ with significant $\prod_{i=1}^P \eta_i(\gamma_i)$. This can be achieved by solving a ranked assignment problem

$$\text{tr}(\mathbf{S}^T \mathbf{C}) = \sum_{i=1}^P \sum_{j=1}^{M+2P} \mathbf{C}_{i,j}\mathbf{S}_{i,j}, \quad (34)$$

$$\mathbf{S}_{i,j} = 1_{\{1:M\}}(j)\delta_{\gamma_i}(j) + \delta_{M+i}(j)\delta_{\gamma_i}(0) + \delta_{M+P+i}(j)\delta_{\gamma_i}(-1), \quad (35)$$

$$\mathbf{C}_{i,j} = \begin{cases} -\ln \eta_i(j), & j \in \{1:M\} \\ -\ln \eta_i(0), & j = M+i \\ -\ln \eta_i(-1), & j = M+P+i \\ \infty, & \text{otherwise} \end{cases} \quad (36)$$

where $\mathbf{S}_{i,j}$ is an assignment matrix, and $\mathbf{C}_{i,j}$ an extended cost matrix. Each γ corresponds to an $\mathbf{S}$, $\text{tr}(\mathbf{S}^T \mathbf{C})$ is the cost of $\mathbf{S}$, and $\exp(-\text{tr}(\mathbf{S}^T \mathbf{C})) = \prod_{i=1}^P \eta_i(\gamma_i)$. Here, we use Gibbs sampling to solve this ranked assignment problem.

We regard each γ as a realization of a random variable that obeys the probability distribution π on $\{-1:M\}^P$. By sampling from π, candidate γ are generated. π is constructed as follows

$$\pi(\gamma) \propto 1_{\dot{\Gamma}}(\gamma)\prod_{i=1}^P \eta_i(\gamma_i). \quad (37)$$

Since it is very difficult to sample directly from the above distribution, the Gibbs sampler is used. We start from an initial solution $\gamma = (\gamma_{1:P})$, and the next solution $\gamma' = (\gamma'_{1:P})$ can be obtained by sampling from a series of conditional distributions $\pi_n(\gamma'_n \mid \gamma'_{1:n-1}, \gamma_{n+1:P})$, $n \in \{1:P\}$, where $\gamma'_{1:n-1}$ and $\gamma_{n+1:P}$ are the newly sampled associations and the associations from the previous solution, respectively. Although the Gibbs sampler is computationally efficient, it requires that the conditional distributions be easily computed and sampled. Therefore, we here provide a closed form expression for each conditional distribution so that they can be calculated or sampled at a low cost. For each $n \in \{1:P\}$,

$$\pi_n(\gamma_n \mid \gamma_{\bar{n}}) \propto \eta_n(\gamma_n)\prod_{i \in \bar{n}}(1 - 1_{\{1:M\}}(\gamma_n)\delta_{\gamma_n}(\gamma_i)) \quad (38)$$

where $\bar{n} = \{1:P\} - \{n\}$, $\gamma_{\bar{n}} = (\gamma_{1:n-1}, \gamma_{n+1:P})$. Then, for

a non-positive j, $\pi_n(j \mid \gamma_{\bar{n}}) \propto \eta_n(j)$, and for $j \in \{1:M\}$, $\pi_n(j \mid \gamma_{\bar{n}}) \propto \eta_n(j)(1 - 1_{\{\gamma'_{1:n-1}, \gamma_{n+1:P}\}}(j))$. Thus, sampling from the conditional distributions is easy and cheap. It only has a linear complexity in the number of measurement partition cells. Finally, given that Gibbs sampling may return the same hypotheses, copies must be removed.

4. ET-BGBP-GP-FLMB Filter

In this section, the BGBP-GP implementation of the ET-FLMB filter is given, and its key is the derivation of likelihood function. Therefore, the specific form of likelihood function is presented first.

4.1 Measurement Likelihood Function

Since the prediction and update of extension state $\mathbf{x}_k^E$ involves operations on high-dimensional vectors and matrices, if $\mathbf{x}_k^E$ is estimated recursively along with the box particles, a lot of running time will be consumed. For real-time consideration, this paper handles the extension state separately in the specific implementation. Thus, the target state can be reconstructed as $\xi_k = (\varepsilon_k, \mathbf{x}_k^E) \triangleq ((D_k, \gamma_k, \mathbf{x}_k^K), \mathbf{x}_k^E)$. In joint prediction and update, only ε_k is calculated. Then, in the GLMB components obtained after joint prediction and update, the position of each hypothesis track is preliminarily extracted and used for the extension state update. In this way, the extension state of each hypothesis track is filtered only once, which can effectively reduce the computational burden. In addition, it should be pointed out that, in joint prediction and update, the correspondences between the hypothesis tracks and the measurement partition cells are saved to facilitate the subsequent extension state update. Based on the above considerations, the measurement likelihood functions of augmented state ε_k and extension state $\mathbf{x}_k^E$ are introduced separately. The likelihood function of augmented state ε_k is presented in the following, and the likelihood function of extension state $\mathbf{x}_k^E$ can be found in Sec. 2.4.

Assuming that the detection set W_k is generated by target ε_k, the measurement likelihood function can be expressed as

$$
\begin{aligned}
p_k(W_k \mid \varepsilon_k) &= p_k(W_k \mid D_k, \gamma_k, \mathbf{x}_k^K) \\
&\propto p_k(W_k \mid D_k) p_k(W_k \mid \gamma_k) p_k(W_k \mid \mathbf{x}_k^K).
\end{aligned} \tag{39}
$$

The above equation is based on the assumption that the detection probability, measurement rate and kinematic state are mutually independent [25]. Under the framework of interval analysis, it can be defined as

$$
p_k([W_k] \mid [\varepsilon_k]) \triangleq p_k(W_k \mid D_k) p_k(|W_k| \| \gamma_k) p_k([W_k] \mid [\mathbf{x}_k^K]) \tag{40}
$$

where $[W_k]$ is the interval measurement formed by W_k, and $|W_k|$ the number of measurements in W_k. $p_k(W_k \mid D_k)$, $p_k(|W_k| \| \gamma_k)$ and $p_k([W_k] \mid [\mathbf{x}_k^K])$ are the likelihood functions of detection probability, measurement rate and kinematic state, respectively.

In this paper, the detection probability is assumed to be an unknown constant, and its likelihood function can be expressed as $p_k(W_k \mid D_k) = \begin{cases} D_k, & W_k \neq \varnothing \\ 1 - D_k, & W_k = \varnothing \end{cases}$. Poisson distribution is used to model the number of measurements produced by each target, so the likelihood function of measurement rate can be expressed as $p_k(|W_k| \| \gamma_k) = \gamma_k^{|W_k|} \mathrm{e}^{-\gamma_k} / |W_k|!$. The likelihood function of kinematic state is defined as $p_k([W_k] \mid [\mathbf{x}_k^K]) \triangleq |[h_{CP}]([\mathbf{x}_k^K], [W_k], [\mathbf{v}_k])| / |[\mathbf{x}_k^K]|$, where $|[\mathbf{x}_k^K]|$ denotes the area of box particle $[\mathbf{x}_k^K]$, and $|[h_{CP}]([\mathbf{x}_k^K], [W_k], [\mathbf{v}_k])|$ the area of the box particle contracted by $[W_k]$ [17]. Finally, $p_k([W_k] \mid [\varepsilon_k])$ can be written as

$$
p_k([W_k] \mid [\varepsilon_k]) =
\begin{cases}
D_k \dfrac{\gamma_k^{|W_k|} \mathrm{e}^{-\gamma_k}}{|W_k|!} \cdot \dfrac{|[h_{CP}]([\mathbf{x}_k^K], [W_k], [\mathbf{v}_k])|}{|[\mathbf{x}_k^K]|}, & W_k \neq \varnothing, \\[4mm]
1 - D_k, & W_k = \varnothing.
\end{cases} \tag{41}
$$

4.2 The BGBP-GP Implementation of the ET-FLMB Filter

(1) *Measurement pretreatment:* Same as our previous work [17], the measurement pretreatment step also includes clutter measurement elimination, measurement partition and box measurement generation. Among them, clutter measurement elimination and measurement partition are identical to [17]. In this work, we also use $\tilde{Z}_k$ to denote the measurement set after clutter removal, and $W_k^{(p,l)}$ to denote the lth measurement partition cell of the pth partition. Since the measurement model is different from [17], the box measurement generation method is different from [17]. The box measurement $[W_k^{(p,l)}]$ corresponding to the cell $W_k^{(p,l)}$ is generated as follows

$$
\begin{aligned}
[W_k^{(p,l)}] &\triangleq ([W_{x,k}^{(p,l)}], [W_{y,k}^{(p,l)}])^T = \\
&([\underline{W_{x,k}^{(p,l)}}, \overline{W_{x,k}^{(p,l)}}], [\underline{W_{y,k}^{(p,l)}}, \overline{W_{y,k}^{(p,l)}}])^T,
\end{aligned} \tag{42}
$$

$$
\underline{W_{x,k}^{(p,l)}} = \min\{\mathbf{z}_{x,k}\} - 3\sigma_x , \quad \overline{W_{x,k}^{(p,l)}} = \max\{\mathbf{z}_{x,k}\} + 3\sigma_x , \tag{43}
$$

$$
\underline{W_{y,k}^{(p,l)}} = \min\{\mathbf{z}_{y,k}\} - 3\sigma_y , \quad \overline{W_{y,k}^{(p,l)}} = \max\{\mathbf{z}_{y,k}\} + 3\sigma_y \tag{44}
$$

where $\mathbf{z}_k \triangleq (\mathbf{z}_{x,k}, \mathbf{z}_{y,k})^T$, $\mathbf{z}_k \in W_k^{(p,l)}$, σ_x and σ_y denote the standard deviation of measurement noise on the X-axis and Y-axis respectively.

(2) *Joint prediction and update:* In this step, we first complete the joint prediction and update of augmented state ε_k, and then predict and update the extension state $\mathbf{x}_k^{\mathrm{E}}$ in the obtained GLMB components.

① *Joint prediction and update of augmented state ε_k:* Suppose that the multiple extended target posterior density at time $k-1$ can be expressed as an LMB RFS with parameter set $\boldsymbol{\pi}_{k-1} = \{(r_{k-1}^{(\mathbf{l}_{k-1})}, p_{k-1}^{(\mathbf{l}_{k-1})})\}_{\mathbf{l}_{k-1} \in \mathbb{L}_{k-1}}$, where $p_{k-1}^{(\mathbf{l}_{k-1})}$ is approximated by a weighted beta gamma box particle set $\{(w_{i,k-1}(\mathbf{l}_{k-1}), [\varepsilon_{i,k-1}(\mathbf{l}_{k-1})])\}_{i=1}^{N_{k-1}(\mathbf{l}_{k-1})}$, i.e.,

$$p_{k-1}^{(\mathbf{l}_{k-1})}(\varepsilon_{k-1}) \approx \sum_{i=1}^{N_{k-1}(\mathbf{l}_{k-1})} w_{i,k-1}(\mathbf{l}_{k-1}) U_{[\varepsilon_{i,k-1}(\mathbf{l}_{k-1})]}(\varepsilon_{k-1}) \quad (45)$$

where $U_{[\cdot]}(\cdot)$ denotes the uniform probability density function over $[\cdot]$. Suppose that the newborn multiple extended target density at time k can be expressed as an LMB RFS with parameter set $\boldsymbol{\pi}_{B,k} = \{(r_{B,k}^{(\mathbf{l}_k)}, p_{B,k}^{(\mathbf{l}_k)})\}_{\mathbf{l}_k \in \mathbb{B}_k}$, where $p_{B,k}^{(\mathbf{l}_k)}$ is approximated by a weighted beta gamma box particle set $\{(w_{B,i,k}(\mathbf{l}_k), [\varepsilon_{B,i,k}(\mathbf{l}_k)])\}_{i=1}^{B_k(\mathbf{l}_k)}$, i.e.,

$$p_{B,k}^{(\mathbf{l}_k)}(\varepsilon_k) \approx \sum_{i=1}^{B_k(\mathbf{l}_k)} w_{B,i,k}(\mathbf{l}_k) U_{[\varepsilon_{B,i,k}(\mathbf{l}_k)]}(\varepsilon_k). \quad (46)$$

Then, the multiple extended target posterior density after joint prediction and update at time k can be expressed as

$$\boldsymbol{\pi}_k(\mathbf{X}_k \mid Z_k) = \Delta(\mathbf{X}_k) \cdot$$
$$\sum_{I_k \in \mathcal{F}(\mathbb{L}_k)} \sum_{i=1}^{|\mathbf{X}_k|+1} \sum_{\substack{\mathcal{U}(Z_k) \in \mathcal{P}_i(Z_k) \\ \theta \in \Theta(\mathcal{U}(Z_k))}} w_{\mathcal{U}(Z_k)}^{(I_k,\theta)} \delta_{I_k}(\mathcal{L}(\mathbf{X}_k)) [p_k^{(\theta)}(\cdot \mid \mathcal{U}(Z_k))]^{\mathbf{X}_k}. \quad (47)$$

In this equation, the weight $w_{\mathcal{U}(Z_k)}^{(I_k,\theta)}$ is calculated as follows

$$w_{\mathcal{U}(Z_k)}^{(I_k,\theta)} \propto 1_{\Theta(I_k)}(\theta) [1 - r_{k-1} \eta_{S,k|k-1}]^{\mathbb{L}_{k-1} - I_k} \cdot$$
$$[r_{k-1} \eta_{S,k|k-1}]^{\mathbb{L}_{k-1} \cap I_k} [1 - r_{B,k}]^{\mathbb{B}_k - I_k} [r_{B,k}]^{\mathbb{B}_k \cap I_k} [\overline{\psi}_{\mathcal{U}(Z_k)}^{(\theta)}]^{I_k}, \quad (48)$$

$$\eta_{S,k|k-1}(\mathbf{l}_k) = \sum_{i=1}^{N_{k-1}(\mathbf{l}_{k-1})} w_{i,k-1}(\mathbf{l}_{k-1}) p_{S,k}([\varepsilon_{i,k-1}(\mathbf{l}_{k-1})], \mathbf{l}_{k-1}), \quad (49)$$

$$\overline{\psi}_{\mathcal{U}(Z_k)}^{(\theta)}(\mathbf{l}_k) = \sum_{i=1}^{N_{k|k-1}(\mathbf{l}_k)} w_{i,k|k-1}(\mathbf{l}_k) \psi_{\mathcal{U}(\tilde{Z}_k)}([\varepsilon_{i,k|k-1}(\mathbf{l}_k)], \mathbf{l}_k; \theta), \quad (50)$$

$$p_{k|k-1}^{(\mathbf{l}_k)}(\varepsilon_k) = \sum_{i=1}^{N_{k|k-1}(\mathbf{l}_k)} w_{i,k|k-1}(\mathbf{l}_k) U_{[\varepsilon_{i,k|k-1}(\mathbf{l}_k)]}(\varepsilon_k)$$
$$= 1_{\mathbb{L}_{k-1}}(\mathbf{l}_k) \sum_{i=1}^{N_{S,k|k-1}(\mathbf{l}_k)} w_{S,i,k|k-1}(\mathbf{l}_k) U_{[\varepsilon_{S,i,k|k-1}(\mathbf{l}_k)]}(\varepsilon_k) \quad (51)$$
$$+ 1_{\mathbb{B}_k}(\mathbf{l}_k) \sum_{i=1}^{N_{B,k}(\mathbf{l}_k)} w_{B,i,k} U_{[\varepsilon_{B,i,k}(\mathbf{l}_k)]}(\varepsilon_k),$$

$$w_{S,i,k|k-1}(\mathbf{l}_k) = \frac{w_{i,k-1}(\mathbf{l}_{k-1}) p_{S,k}([\varepsilon_{i,k-1}(\mathbf{l}_{k-1})], \mathbf{l}_{k-1})}{\sum_{j=1}^{N_{k-1}(\mathbf{l}_{k-1})} w_{j,k-1}(\mathbf{l}_{k-1}) p_{S,k}([\varepsilon_{j,k-1}(\mathbf{l}_{k-1})], \mathbf{l}_{k-1})} \quad (52)$$

where $[\varepsilon_{i,k|k-1}(\mathbf{l}_k)]$ is the predicted beta gamma box particle, and $\psi_{\mathcal{U}(\tilde{Z}_k)}([\varepsilon_{i,k|k-1}(\mathbf{l}_k)], \mathbf{l}_k; \theta)$ the likelihood function. They can be calculated as follows

$$[\varepsilon_{i,k|k-1}(\mathbf{l}_k)] = [(D_{i,k|k-1}(\mathbf{l}_k), \gamma_{i,k|k-1}(\mathbf{l}_k), \mathbf{x}_{i,k|k-1}^{\mathrm{K}}(\mathbf{l}_k))]$$
$$= (D_{i,k|k-1}(\mathbf{l}_k), \gamma_{i,k|k-1}(\mathbf{l}_k), [\mathbf{x}_{i,k|k-1}^{\mathrm{K}}(\mathbf{l}_k)]), \quad (53)$$

$$D_{i,k|k-1}(\mathbf{l}_k) = s_{i,k|k-1}(\mathbf{l}_k) / (s_{i,k|k-1}(\mathbf{l}_k) + t_{i,k|k-1}(\mathbf{l}_k)), \quad (54)$$

$$s_{i,k|k-1}(\mathbf{l}_k) = \left(\frac{\mu_{i,\beta,k|k-1}(\mathbf{l}_k)(1 - \mu_{i,\beta,k|k-1}(\mathbf{l}_k))}{(\sigma_{i,\beta,k|k-1}(\mathbf{l}_k))^2} - 1 \right) \mu_{i,\beta,k|k-1}(\mathbf{l}_k), \quad (55)$$

$$t_{i,k|k-1}(\mathbf{l}_k) = \left(\frac{\mu_{i,\beta,k|k-1}(\mathbf{l}_k)(1 - \mu_{i,\beta,k|k-1}(\mathbf{l}_k))}{(\sigma_{i,\beta,k|k-1}(\mathbf{l}_k))^2} - 1 \right)(1 - \mu_{i,\beta,k|k-1}(\mathbf{l}_k)), \quad (56)$$

$$\mu_{i,\beta,k|k-1}(\mathbf{l}_k) = \mu_{i,\beta,k-1}(\mathbf{l}_{k-1}) = \frac{s_{i,k-1}(\mathbf{l}_{k-1})}{s_{i,k-1}(\mathbf{l}_{k-1}) + t_{i,k-1}(\mathbf{l}_{k-1})}, \quad (57)$$

$$(\sigma_{i,\beta,k|k-1}(\mathbf{l}_k))^2 = \upsilon_D (\sigma_{i,\beta,k-1}(\mathbf{l}_{k-1}))^2 =$$
$$\upsilon_D \frac{s_{i,k-1}(\mathbf{l}_{k-1}) t_{i,k-1}(\mathbf{l}_{k-1})}{(s_{i,k-1}(\mathbf{l}_{k-1}) + t_{i,k-1}(\mathbf{l}_{k-1}))^2 (s_{i,k-1}(\mathbf{l}_{k-1}) + t_{i,k-1}(\mathbf{l}_{k-1}) + 1)}, \quad (58)$$

$$\gamma_{i,k|k-1}(\mathbf{l}_k) = \alpha_{i,k|k-1}(\mathbf{l}_k) / \beta_{i,k|k-1}(\mathbf{l}_k), \quad (59)$$

$$\alpha_{i,k|k-1}(\mathbf{l}_k) = \alpha_{i,k-1}(\mathbf{l}_{k-1}) / \eta_\gamma, \quad \beta_{i,k|k-1}(\mathbf{l}_k) = \beta_{i,k-1}(\mathbf{l}_{k-1}) / \eta_\gamma, \quad (60)$$

$$[\mathbf{x}_{i,k|k-1}^{\mathrm{K}}(\mathbf{l}_k)] = [f_{\mathbf{x}^{\mathrm{K}},k|k-1}]([\mathbf{x}_{i,k-1}^{\mathrm{K}}(\mathbf{l}_{k-1})]) + [\mathbf{w}_{i,k}^{\mathrm{K}}], \quad (61)$$

$$\psi_{\mathcal{U}(\tilde{Z}_k)}([\varepsilon_{i,k|k-1}(\mathbf{l}_k)], \mathbf{l}_k; \theta) =$$
$$\begin{cases} \dfrac{D_{i,k|k-1}(\mathbf{l}_k) \tilde{g}([\mathcal{U}_{\theta(\mathbf{l}_k)}(\tilde{Z}_k)] \mid (\gamma_{i,k|k-1}(\mathbf{l}_k), [\mathbf{x}_{i,k|k-1}^{\mathrm{K}}(\mathbf{l}_k)]), \mathbf{l}_k)}{[\kappa]^{[\mathcal{U}_{\theta(\mathbf{l}_k)}(\tilde{Z}_k)]}}, & \theta(\mathbf{l}_k) > 0, \\ 1 - D_{i,k|k-1}(\mathbf{l}_k), & \theta(\mathbf{l}_k) = 0, \end{cases} \quad (62)$$

$$\tilde{g}([\mathcal{U}_{\theta(\mathbf{l}_k)}(\tilde{Z}_k)] \mid (\gamma_{i,k|k-1}(\mathbf{l}_k), [\mathbf{x}_{i,k|k-1}^{\mathrm{K}}(\mathbf{l}_k)]), \mathbf{l}_k) =$$
$$\frac{\gamma_{k|k-1}^{|\mathcal{U}_{\theta(\mathbf{l}_k)}(\tilde{Z}_k)|} \mathrm{e}^{-\gamma_{k|k-1}}}{|\mathcal{U}_{\theta(\mathbf{l}_k)}(\tilde{Z}_k)|!} \cdot \frac{|[h_{CP}]([\mathbf{x}_{i,k|k-1}^{\mathrm{K}}(\mathbf{l}_k)], [\mathcal{U}_{\theta(\mathbf{l}_k)}(\tilde{Z}_k)], [\mathbf{v}_k])|}{|[\mathbf{x}_{i,k|k-1}^{K}(\mathbf{l}_k)]|}. \quad (63)$$

In the above equations, $[\mathcal{U}_{\theta(\mathbf{l}_k)}(\tilde{Z}_k)]$ denotes the box measurement corresponding to the cell $\mathcal{U}_{\theta(\mathbf{l}_k)}(\tilde{Z}_k)$, and it is equivalent to a box measurement $[W_k^{(p,l)}]$ formed in the measurement pretreatment. After that, the single target probability density $p_k^{(\theta)}(\cdot \mid \mathcal{U}(Z_k))$ in (47) is calculated as follows

$$p_k^{(\theta)}(\varepsilon_k, \mathbf{l}_k \mid \mathcal{U}(\tilde{Z}_k)) = \sum_{i=1}^{N_k(\mathbf{l}_k)} w_{i,k}(\mathbf{l}_k) U_{[\varepsilon_{i,k}(\mathbf{l}_k)]}(\varepsilon_k), \quad (64)$$

$$w_{i,k}(\mathbf{l}_k) = w_{i,k|k-1}(\mathbf{l}_k) \psi_{\mathcal{U}(\tilde{Z}_k)}([\varepsilon_{i,k|k-1}(\mathbf{l}_k)], \mathbf{l}_k; \theta) / \overline{\psi}_{\mathcal{U}(Z_k)}^{(\theta)}(\mathbf{l}_k) \quad (65)$$

where $[\varepsilon_{i,k}(\mathbf{l}_k)]$ is the updated beta gamma box particle. It can be calculated as follows

$$[\varepsilon_{i,k}(\mathbf{l}_k)] = [(D_{i,k}(\mathbf{l}_k), \gamma_{i,k}(\mathbf{l}_k), \mathbf{x}_{i,k}^{\mathrm{K}}(\mathbf{l}_k))] \\ = (D_{i,k}(\mathbf{l}_k), \gamma_{i,k}(\mathbf{l}_k), [\mathbf{x}_{i,k}^{\mathrm{K}}(\mathbf{l}_k)]), \quad (66)$$

$$D_{i,k}(\mathbf{l}_k) = s_{i,k}(\mathbf{l}_k) / (s_{i,k}(\mathbf{l}_k) + t_{i,k}(\mathbf{l}_k)), \quad (67)$$

$$s_{i,k}(\mathbf{l}_k) = \begin{cases} s_{i,k|k-1}(\mathbf{l}_k), & \theta(\mathbf{l}_k) = 0, \\ s_{i,k|k-1}(\mathbf{l}_k) + 1, & \theta(\mathbf{l}_k) > 0, \end{cases} \quad (68)$$

$$t_{i,k}(\mathbf{l}_k) = \begin{cases} t_{i,k|k-1}(\mathbf{l}_k) + 1, & \theta(\mathbf{l}_k) = 0, \\ t_{i,k|k-1}(\mathbf{l}_k), & \theta(\mathbf{l}_k) > 0, \end{cases} \quad (69)$$

$$\gamma_{i,k}(\mathbf{l}_k) = \alpha_{i,k}(\mathbf{l}_k) / \beta_{i,k}(\mathbf{l}_k), \quad (70)$$

$$\alpha_{i,k}(\mathbf{l}_k) = \alpha_{i,k|k-1}(\mathbf{l}_k) + |\mathcal{U}_{\theta_k(\mathbf{l}_k)}(\tilde{Z}_k)|, \quad (71)$$

$$\beta_{i,k}(\mathbf{l}_k) = \beta_{i,k|k-1}(\mathbf{l}_k) + 1, \quad (72)$$

$$[\mathbf{x}_{i,k}^{\mathrm{K}}(\mathbf{l}_k)] = \begin{cases} [\tilde{\mathbf{x}}_{i,k|k-1}^{\mathrm{K}}(\mathbf{l}_k)], \text{if } [h]([\mathbf{x}_{i,k|k-1}^{\mathrm{K}}(\mathbf{l}_k)]) \bigcap [\mathcal{U}_{\theta(\mathbf{l}_k)}(\tilde{Z}_k)] \neq \varnothing \\ [\mathbf{x}_{i,k|k-1}^{\mathrm{K}}(\mathbf{l}_k)], \text{if } [h]([\mathbf{x}_{i,k|k-1}^{\mathrm{K}}(\mathbf{l}_k)]) \bigcap [\mathcal{U}_{\theta(\mathbf{l}_k)}(\tilde{Z}_k)] = \varnothing \end{cases} \quad (73)$$

where $[h]$ is the inclusion function corresponding to h, and $[\tilde{\mathbf{x}}_{i,k|k-1}^{\mathrm{K}}(\mathbf{l}_k)]$ the contracted version of $[\mathbf{x}_{i,k|k-1}^{\mathrm{K}}(\mathbf{l}_k)]$. Following [17], we also use the CP algorithm to contract $[\mathbf{x}_{i,k|k-1}^{\mathrm{K}}(\mathbf{l}_k)]$. The position dimensions of $[\mathbf{x}_{i,k|k-1}^{\mathrm{K}}(\mathbf{l}_k)]$ are contracted by $[\mathcal{U}_{\theta(\mathbf{l}_k)}(\tilde{Z}_k)]$, and its velocity dimensions are contracted by the preset velocity intervals. Finally, it should be emphasized that, in (47), the hypothesis components with larger weights are computed by the extended cost matrix and Gibbs sampling, which can be seen in Sec. 3.2.

② *Prediction and update of extension state* $\mathbf{x}_k^{\mathrm{E}}$: Each hypothesis track in the GLMB components obtained after joint prediction and update not only contains the updated beta gamma box particle set, but also saves the extension state of the extended target at the last moment and the measurement partition cell corresponding to the extended target. Here, we consider a given hypothesis track $(\xi_k', \mathbf{l}_k)$ and its corresponding measurement partition cell $\mathcal{U}_{\theta(\mathbf{l}_k)}(\tilde{Z}_k)$, where $\xi_k' = (\varepsilon_k, \mathbf{x}_{k-1}^{\mathrm{E}}) = ((D_k, \gamma_k, \mathbf{x}_k^{\mathrm{K}}), \mathbf{x}_{k-1}^{\mathrm{E}})$, $\mathcal{U}_{\theta(\mathbf{l}_k)}(\tilde{Z}_k) = \{z_{k,j}\}_{j=1}^{|\mathcal{U}_{\theta(\mathbf{l}_k)}(\tilde{Z}_k)|}$, $\mathbf{x}_k^{\mathrm{K}}$ can be approximated by $\overline{\mathbf{x}}_k^{\mathrm{K}} = \sum_{i=1}^{N_k(\mathbf{l}_k)} w_{i,k}\mathrm{mid}([\mathbf{x}_{i,k}^{\mathrm{K}}(\mathbf{l}_k)])$, $\overline{\mathbf{x}}_k^c = (\overline{\mathbf{x}}_{x,k}^{\mathrm{K}}, \overline{\mathbf{x}}_{y,k}^{\mathrm{K}})^{\mathrm{T}}$, and $\mathrm{mid}(\cdot)$ is the function to compute the box particle center.

The extension state can be filtered by the extended Kalman filter (EKF). Its prediction step is as follows

$$\mathbf{x}_{k|k-1}^{\mathrm{E}} = \mathbf{F}^{\mathrm{E}}\mathbf{x}_{k-1}^{\mathrm{E}}, \quad \mathbf{P}_{k|k-1}^{\mathrm{E}} = \mathbf{F}^{\mathrm{E}}\mathbf{P}_{k-1}^{\mathrm{E}}(\mathbf{F}^{\mathrm{E}})^{\mathrm{T}} + \mathbf{Q}^{\mathrm{E}}. \quad (74)$$

Its update step is as follows

$$\mathbf{z}_{\mathcal{U}_{\theta(\mathbf{l}_k)}(\tilde{Z}_k)} \triangleq \bigoplus_{j=1,\cdots,|\mathcal{U}_{\theta(\mathbf{l}_k)}(\tilde{Z}_k)|} \mathbf{z}_{k,j}, \quad (75)$$

$$\mathbf{z}_{k|k-1, \mathcal{U}_{\theta(\mathbf{l}_k)}(\tilde{Z}_k)} \triangleq \bigoplus_{j=1,\cdots,|\mathcal{U}_{\theta(\mathbf{l}_k)}(\tilde{Z}_k)|} \mathbf{z}_{k|k-1,j}, \quad (76)$$

$$\mathbf{H}_{\mathcal{U}_{\theta(\mathbf{l}_k)}(\tilde{Z}_k)}^{\mathrm{E}} \triangleq ((\overline{\mathbf{H}}_{k,1}^{\mathrm{E}})^{\mathrm{T}}, \cdots, (\overline{\mathbf{H}}_{k,j}^{\mathrm{E}})^{\mathrm{T}}, \cdots, (\overline{\mathbf{H}}_{k,|\mathcal{U}_{\theta(\mathbf{l}_k)}(\tilde{Z}_k)|}^{\mathrm{E}})^{\mathrm{T}})^{\mathrm{T}}, \quad (77)$$

$$\mathbf{R}_{\mathcal{U}_{\theta(\mathbf{l}_k)}(\tilde{Z}_k)} \triangleq \mathrm{blkdiag}(\overline{\mathbf{R}}_{k,1}, \cdots, \overline{\mathbf{R}}_{k,j}, \cdots, \overline{\mathbf{R}}_{k,|\mathcal{U}_{\theta(\mathbf{l}_k)}(\tilde{Z}_k)|}), \quad (78)$$

$$\mathbf{z}_{k|k-1,j} = h_{k,j}(\overline{\mathbf{x}}_k^c, \mathbf{x}_{k|k-1}^{\mathrm{E}}) = \overline{\mathbf{x}}_k^c + \mathbf{p}_k^{\mathrm{E}}(\theta_{k,j}^{\mathrm{E}})\mathbf{H}_k^{\mathrm{E}}(\theta_{k,j}^{\mathrm{E}})\mathbf{x}_{k|k-1}^{\mathrm{E}}, \quad (79)$$

$$\overline{\mathbf{H}}_{k,j}^{\mathrm{E}} = \frac{\mathrm{d}}{\mathrm{d}\mathbf{x}_k^{\mathrm{E}}} h_{k,j}(\overline{\mathbf{x}}_k^c, \mathbf{x}_k^{\mathrm{E}})|_{\mathbf{x}_k^{\mathrm{E}}=\mathbf{x}_{k|k-1}^{\mathrm{E}}} = \mathbf{p}_k^{\mathrm{E}}(\theta_{k,j}^{\mathrm{E}})\mathbf{H}_k^{\mathrm{E}}(\theta_{k,j}^{\mathrm{E}}), \quad (80)$$

$$\mathbf{S}_{k|k-1}^{\mathrm{E}} = \mathbf{H}_{\mathcal{U}_{\theta(\mathbf{l}_k)}(\tilde{Z}_k)}^{\mathrm{E}} \mathbf{P}_{k|k-1}^{\mathrm{E}} (\mathbf{H}_{\mathcal{U}_{\theta(\mathbf{l}_k)}(\tilde{Z}_k)}^{\mathrm{E}})^{\mathrm{T}} + \mathbf{R}_{\mathcal{U}_{\theta(\mathbf{l}_k)}(\tilde{Z}_k)}, \quad (81)$$

$$\mathbf{K}_k^{\mathrm{E}} = \mathbf{P}_{k|k-1}^{\mathrm{E}} (\mathbf{H}_{\mathcal{U}_{\theta(\mathbf{l}_k)}(\tilde{Z}_k)}^{\mathrm{E}})^{\mathrm{T}} (\mathbf{S}_{k|k-1}^{\mathrm{E}})^{-1}, \quad (82)$$

$$\mathbf{x}_k^{\mathrm{E}} = \mathbf{x}_{k|k-1}^{\mathrm{E}} + \mathbf{K}_k^{\mathrm{E}}(\mathbf{z}_{\mathcal{U}_{\theta(\mathbf{l}_k)}(\tilde{Z}_k)} - \mathbf{z}_{k|k-1, \mathcal{U}_{\theta(\mathbf{l}_k)}(\tilde{Z}_k)}), \quad (83)$$

$$\mathbf{P}_k^{\mathrm{E}} = \mathbf{P}_{k|k-1}^{\mathrm{E}} + \mathbf{K}_k^{\mathrm{E}}\mathbf{H}_{\mathcal{U}_{\theta(\mathbf{l}_k)}(\tilde{Z}_k)}^{\mathrm{E}} \mathbf{P}_{k|k-1}^{\mathrm{E}} \quad (84)$$

where $\oplus$ denotes the vertical vectorial concatenation. Thus, the updated extension state $\mathbf{x}_k^{\mathrm{E}}$ of track $\mathbf{l}_k$ is obtained.

③ *Approximating GLMB as LMB:* Finally, in order to close the recursion, the obtained GLMB density needs to be approximated as LMB. The calculation of the transformed LMB parameters can be seen in Sec. 3.2, and the extension state takes the weighted average result of different hypothesis components.

(3) *Track pruning, truncation and resampling:* After joint prediction and update, the LMB components need to be pruned, truncated and resampled. The pruning and truncation methods are the same as the ET-LMB filter [8]. The box particle resampling adopts the division resampling strategy presented in [1], but it should be noted that the detection probability and measurement rate parameters are directly copied in this process.

(4) *State estimation:* The number of extended targets is estimated according to the maximum a posteriori (MAP) criterion, i.e., $\hat{N}_k = \arg\max_n \rho_k(n)$, where $\rho_k(n)$ is the cardinality distribution of LMB parameter set [3]. The extended target states are estimated as

$$\hat{\mathbf{X}}_k = \{(\hat{\xi}_k^{(j)}, \hat{\mathbf{l}}_k^{(j)})\}_{j=1}^{\hat{N}_k}, \quad (85)$$

$$\hat{\xi}_k^{(j)} = ((\hat{D}_k^{(j)}, \hat{\gamma}_k^{(j)}, \hat{\mathbf{x}}_k^{\mathrm{K},(j)}), \hat{\mathbf{x}}_k^{\mathrm{E},(j)}), \hat{\mathbf{l}}_k^{(j)} \in I_k, \quad (86)$$

$$\hat{D}_k^{(j)} = \sum_{i=1}^{N_k(\mathbf{l}_k)} w_{i,k}^{(j)} D_{i,k}^{(j)}(\mathbf{l}_k^{(j)}), \quad \hat{\gamma}_k^{(j)} = \sum_{i=1}^{N_k(\mathbf{l}_k)} w_{i,k}^{(j)} \gamma_{i,k}^{(j)}(\mathbf{l}_k^{(j)}), \quad (87)$$

$$\hat{\mathbf{x}}_k^{\mathrm{K},(j)} = \sum_{i=1}^{N_k(\mathbf{l}_k)} w_{i,k}^{(j)} \mathrm{mid}([\mathbf{x}_{i,k}^{\mathrm{K},(j)}(\mathbf{l}_k^{(j)})]), \quad \hat{\mathbf{x}}_k^{\mathrm{E},(j)} = \mathbf{x}_k^{\mathrm{E},(j)}(\mathbf{l}_k^{(j)}). \quad (88)$$

4.3 Performance Evaluation Criteria

This paper uses the OSPA distance [26] to evaluate the estimation performance of multiple extended target detection probabilities, measurement rates, kinematic states and extension states. The original OSPA distance is defined as follows

$$
\bar{d}_p^{(c)}(\mathbf{X}, \hat{\mathbf{X}}) =
\begin{cases}
0, & m = n = 0 \\
(\frac{1}{n}(\min_{\pi \in \prod_n} \sum_{i=1}^m d^{(c)}(x_i, \hat{x}_{\pi(i)})^p + c^p(n-m)))^{\frac{1}{p}}, & m \le n \\
\bar{d}_p^{(c)}(\hat{\mathbf{X}}, \mathbf{X}), & m > n
\end{cases} \quad (89)
$$

where $\mathbf{X} = \{x_1, x_2, \cdots, x_m\}$ denotes the real extended target state set, $\hat{\mathbf{X}} = \{\hat{x}_1, \hat{x}_2, \cdots, \hat{x}_n\}$ the estimated extended target state set, c the cutoff distance, and $\prod_n$ all permutations on $\{1, 2, \cdots, n\}$. In this paper, the real target state set and the estimated target state set are $\{(\xi_k^{(i)}, \mathbf{l}_k^{(i)})\}_{i=1}^{N_k}$ and $\{(\hat{\xi}_k^{(j)}, \hat{\mathbf{l}}_k^{(j)})\}_{j=1}^{\hat{N}_k}$ respectively, where $\xi_k^{(i)} = ((D_k^{(i)}, \gamma_k^{(i)}, \mathbf{x}_k^{K,(i)}), \mathbf{x}_k^{E,(i)})$, $\hat{\xi}_k^{(j)} = ((\hat{D}_k^{(j)}, \hat{\gamma}_k^{(j)}, \hat{\mathbf{x}}_k^{K,(j)}), \hat{\mathbf{x}}_k^{E,(j)})$. For the detection probabilities, measurement rates, kinematic states and extension states, $d^{(c)}(x_i, \hat{x}_{\pi(i)})$ in (89) is respectively defined as follows

$$
d^{(c_D)}(D_k^{(i)}, \hat{D}_k^{(\pi(i))}) \triangleq \min(c_D, |D_k^{(i)} - \hat{D}_k^{(\pi(i))}|), \quad (90)
$$

$$
d^{(c_\gamma)}(\gamma_k^{(i)}, \hat{\gamma}_k^{(\pi(i))}) \triangleq \min(c_\gamma, |\gamma_k^{(i)} - \hat{\gamma}_k^{(\pi(i))}|), \quad (91)
$$

$$
d^{(c_{\mathbf{x}^K})}(\mathbf{x}_k^{K,(i)}, \hat{\mathbf{x}}_k^{K,(\pi(i))}) \triangleq \min(c_{\mathbf{x}^K}, \|\mathbf{x}_k^{K,(i)} - \hat{\mathbf{x}}_k^{K,(\pi(i))}\|), \quad (92)
$$

$$
d^{(c_{\mathbf{x}^E})}(\mathbf{x}_k^{E,(i)}, \hat{\mathbf{x}}_k^{E,(\pi(i))}) \triangleq \min(c_{\mathbf{x}^E}, \|\mathbf{x}_k^{E,(i)} - \hat{\mathbf{x}}_k^{E,(\pi(i))}\|) \quad (93)
$$

where $|\cdot|$ is the absolute value, and $\|\cdot\|$ the Euclidean norm.

4.4 Discussions

The main advantages of the proposed filter are as follows.

(1) The ET-LMB filter needs to convert LMB into GLMB before the measurement update, which leads to a large number of the hypothesis components participating in the measurement update. The proposed filter integrates prediction and update into one step, which can avoid the high number of hypothesis components and reduce the amount of computation. In addition, instead of Murty's algorithm, the proposed filter uses Gibbs sampling to calculate the hypothesis components with larger weights, further reducing the computational complexity. The computational complexity of Murty's algorithm is the fourth power of the number of measurement partition cells, while Gibbs sampling has a linear complexity in the number of measurement partition cells [4].

(2) The proposed filter is implemented by box particles. Compared with the traditional SMC implementation, it greatly reduces the number of particles and computational burden.

(3) In the concrete implementation, the detection probability, measurement rate and extension state of each extended target are also estimated recursively. The proposed filter can not only estimate the extension states with arbitrary star-convex shapes, but also be applicable to the case of unknown detection probability. The above advantages are verified in the subsequent simulations.

5. Simulations and Analyses

To verify the effectiveness of the proposed ET-BGBP-GP-FLMB filter, two simulations are set up here, including a linear scenario and a nonlinear scenario. The software platform of simulations is MATLAB R2018b with INTLAB toolbox, and it is installed on the personal computer with Intel(R) Core(TM) i5-8250U CPU @ 1.60 GHz 1.80 GHz processor and 16.0 GB RAM.

5.1 Simulation 1

The algorithms compared in this simulation include the ET-BP-PHD, ET-GSMC-GP-LMB, ET-GBP-GP-LMB, ET-GBP-GP-FLMB and ET-BGBP-GP-FLMB filters. The ET-BP-PHD filter is an upgraded version of the ET-Box-PHD filter [22]. For a fair comparison, the ET-BP-PHD filter adopts the measurement pretreatment method presented in this paper. In addition, the ET-BP-PHD filter adopts an improved *k*-means clustering to improve the extraction effect of target states, that is, the global optimal solution is approximated by the local optimal solution obtained after multiple clustering. The ET-GSMC-GP-LMB filter is the GSMC-GP implementation of the ET-LMB filter, the ET-GBP-GP-LMB filter is the GBP-GP implementation of the ET-LMB filter, and the ET-GBP-GP-FLMB filter is the GBP-GP implementation of the ET-FLMB filter.

This simulation is a linear scenario with surveillance area $[-1000, 1000]$ m $\times$ $[-1000, 1000]$ m. The monitoring duration is 100 s, and the sampling interval is $T = 1$ s. A total of five targets with different shapes appeared successively in the surveillance area. The first target is a rectangle with length 6 m and width 4 m. Its survival time is 1–85 s. The second target is a star-convex shape. Its major axis is 8 m, minor axis is 6 m, and the width of both axes is 2 m. Its survival time is 5–90 s. The third target is an ellipse with major axis 6 m and minor axis 4 m. Its survival time is 10–95 s. The fourth target is a circle with radius 3 m, and its survival time is 15–100 s. The fifth target is a circle with radius 3 m, and its survival time is 20–100 s. The motion of each target is modeled as the constant velocity (CV) model with the following dynamic equation

$$\mathbf{x}_k^K = \mathbf{F}^K \mathbf{x}_{k-1}^K + \mathbf{G}^K \mathbf{w}_{k-1}^K, \tag{94}$$

$$\mathbf{F}^K = \begin{bmatrix} 1 & T & 0 & 0 \\ 0 & 1 & 0 & 0 \\ 0 & 0 & 1 & T \\ 0 & 0 & 0 & 1 \end{bmatrix}, \quad \mathbf{G}^K = \begin{bmatrix} \dfrac{T^2}{2} & T & 0 & 0 \\ 0 & 0 & \dfrac{T^2}{2} & T \end{bmatrix}^T \tag{95}$$

where $\mathbf{x}_k^K \triangleq (\mathbf{x}_{x,k}^K, \dot{\mathbf{x}}_{x,k}^K, \mathbf{x}_{y,k}^K, \dot{\mathbf{x}}_{y,k}^K)^T$, and $\mathbf{w}_{k-1}^K$ is a zero mean Gaussian process noise with the standard deviation $\sigma_{\mathbf{w}_{k-1}^K} = 4$ m/s². The extension state dynamic equation can be found in Sec. 2.2, and the extension state dimension is 50 dimensions, i.e., $N^E = 50$. The GP parameters are $\sigma_r = 2$ m, $\sigma_f = 2$ m, and $l = \pi/8$ rad. The measurement equation is shown in Sec. 2.3. The measurement rate and detection probability of each target are 20 and 0.9999, respectively. The standard deviation of measurement noise is $\sigma_x = \sigma_y = 0.1$ m/s². In the surveillance area, the clutter is evenly distributed, and its number follows Poisson distribution with mean 1. The target survival probability is $p_s = 0.999$.

In the filtering process, the ET-GSMC-GP-LMB filter uses 500 and 2000 particles respectively, and they are denoted as ET-GSMC-GP-LMB-500 and ET-GSMC-GP-LMB-2000. Other filters implemented by box particles use 10 box particles. For newborn targets, this paper adopts the measurement driven method to detect them [17]. In the SMC implementation, 50 particles are sampled to detect newborn targets, while in the box particle implementation, only one box particle is sampled. In addition, in the ET-GSMC-GP-LMB, ET-GBP-GP-LMB, ET-GBP-GP-FLMB and ET-BGBP-GP-FLMB filters, the maximum track number is 100, the track pruning threshold is 1e–3, and the requested number of hypothesis components for GLMB update is 250. Finally, the parameters of the OSPA distance used to evaluate the detection probability, measurement rate, kinematic state and extension state estimation effect are $c_D = 1$ and $p_D = 1$, $c_\gamma = 50$ and $p_\gamma = 1$, $c_{\mathbf{x}^K} = 50$ and $p_{\mathbf{x}^K} = 1$, $c_{\mathbf{x}^E} = 50$ and $p_{\mathbf{x}^E} = 1$, respectively. Note that the parameter c in the OSPA distance is the cutoff distance, which is used to truncate and adjust the influence of cardinality error. Generally, c is taken as 100, or larger or smaller. This paper sets $c = 50$. However, for the OSPA distance parameter c of detection probability, we set $c = 1$. This is because the range of detection probability is 0 to 1, and it is sufficient to truncate with $c = 1$. What's more, the change range of detection probability is small, and it is difficult to observe the change of the detection probability OSPA distance if the cardinality penalty is too large. The single tracking result of the ET-BGBP-GP-FLMB filter is shown in Fig. 2.

In Fig. 2, the black solid lines denote the real tracks and shapes of extended targets, the circles and triangles denote the initial and terminal positions of targets respectively, and different colors denote different labels, which represent the tracking results of different targets. It can be
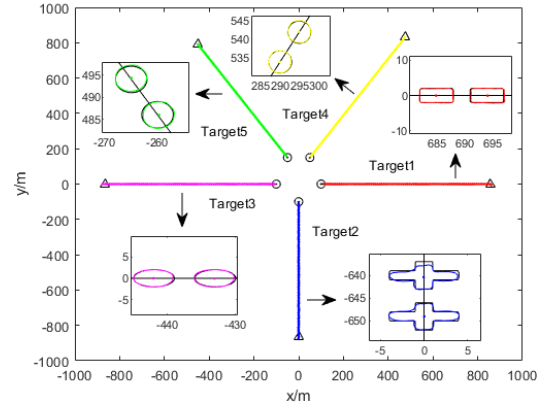

Fig. 2. The single tracking result of the ET-BGBP-GP-FLMB filter.

seen that, the ET-BGBP-GP-FLMB filter can not only effectively estimate the position and extension state of each extended target, but also output their tracks.

The average results of 100 Monte Carlo simulations are shown in Fig. 3 and Tab. 1. It should be pointed out that the proposed filter can estimate the detection probability of each target, so the detection probability estimation is also evaluated by the OSPA distance. Further, considering that the detection probability of each target is the same in this simulation, their average value is calculated as the estimation of detection probability. The real detection probability and estimated detection probability are plotted in Fig. 3(e), which more intuitively shows the estimation effect of detection probability.
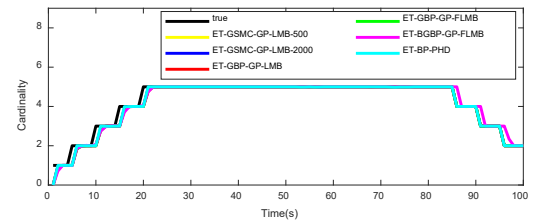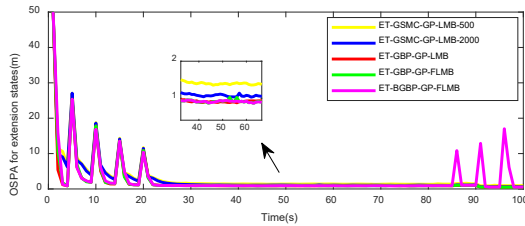

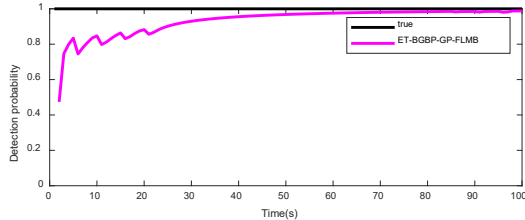(a) The average cardinality estimations.
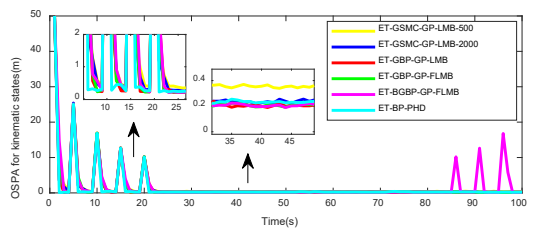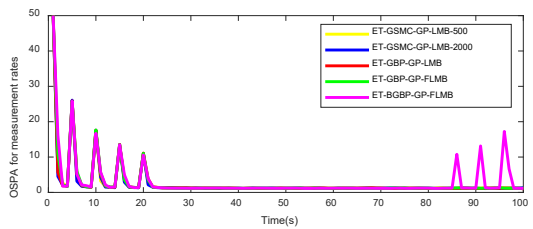
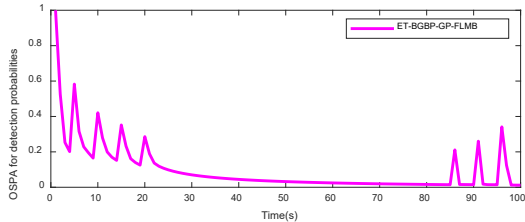(b) The average OSPA distances of kinematic states.

(c) The average OSPA distances of measurement rates.

(d) The average OSPA distances of extension states.

(e) The average detection probability estimation.

(f) The average OSPA distance of detection probabilities.

Fig. 3. The average results of 100 Monte Carlo simulations.

Filter	Run time (s)
ET-GSMC-GP-LMB-500	236.3330
ET-GSMC-GP-LMB-2000	753.7002
ET-GBP-GP-LMB	103.1447
ET-GBP-GP-FLMB	42.1879
ET-BGBP-GP-FLMB	48.5068
ET-BP-PHD	28.3481

Tab. 1. The average running time statistics.

It can be seen from Fig. 3 that, under ideal detection conditions, all filters can obtain good estimation results. The estimation performance of different filters is similar, but there are also some differences. Table 1 shows the average running time of each filter. In the aspect of cardinality estimation, all filters have delays at the target birth moments. This is because the filters use the measurement driven method to detect newborn targets, which requires sampling at the measurement locations at the previous moment. The delays of the proposed filter are slightly longer than that of other filters. This is because the detection probability of each target in the proposed filter is estimated in real-time. The initial detection probabilities of newborn targets are low, which leads to their slower detection. At the target death moments, the cardinality estimation of the proposed filter is delayed. This is also because the detection probability of each target is estimated in real-time. Although the detection probability estimation of each target becomes more and more accurate with the accumulation of measurements, when a target dies, its detection probability estimation may still be less than the survival

probability, resulting in a missed detection cost less than death. Therefore, in the optimal hypothesis component, the target is temporarily judged to be missed. When the measurements are still not detected at the subsequent time, it is determined that the target is dead, and the target number is estimated to decrease. When there are errors in target number estimation, the OSPA distances of kinematic states, measurement rates, extension states and detection probabilities will produce a spike. It can be seen from the local enlargement of Fig. 3(b) and (d) that, the estimation performance of the ET-GSMC-GP-LMB filter is improved with the increase of particle number. However, it can be seen from Tab. 1 that this is at the cost of huge runtime. Compared with the ET-GSMC-GP-LMB filter, the ET-GBP-GP-LMB filter greatly reduces the number of particles and computational burden. Compared with the ET-GBP-GP-LMB filter, the ET-GBP-GP-FLMB filter is based on the ET-FLMB filter proposed in this paper, which greatly reduces the number of hypothesis components and further reduces the computational complexity. On this basis, the proposed ET-BGBP-GP-FLMB filter increases the estimation of the detection probability with a small time cost, and broadens the application range of the filter. It can be seen from Fig. 3(e) that, with the increase of observation time, the average detection probability estimation is getting closer to the real detection probability. The running time of the ET-BP-PHD filter is the least, however, it can only estimate the number and kinematic states of extended targets.

In order to further verify the estimation effect of the proposed ET-BGBP-GP-FLMB filter, the real detection probability is set to 0.88 for simulation, and other parameters remain unchanged. Considering the huge computational burden of the SMC implementation, only the ET-GBP-GP-LMB, ET-GBP-GP-FLMB, ET-BGBP-GP-FLMB and ET-BP-PHD filters are compared here. The average results of 100 Monte Carlo simulations are shown in Fig. 4 and Tab. 2.

It can be seen from Fig. 4 that the estimation performance of the filters decreases when the detection probability is low. However, the estimation performance of ET-BP-PHD filter is greatly reduced, while the estimation performance of the other three filters is similar and the degradation is not significant. This is because the ET-BP-PHD filter is based on traditional RFS, which is the first moment approximation of the multi-target Bayesian filter and a suboptimal solution. Other filters are based on labeled RFS and are approximate solutions under the optimal framework. They can avoid many disadvantages of the ET-BP-PHD filter. At the target death moments, the cardinality estimations of the ET-GBP-GP-LMB, ET-GBP-GP-FLMB and ET-BGBP-GP-FLMB filters are all delayed. This is because, as the detection probability decreases, the possibility of missed detection of each target gradually increases. When a target disappears, the three filters are more likely to temporarily judge the dead target as a missed detection, which is more likely to cause a delay in cardinal-
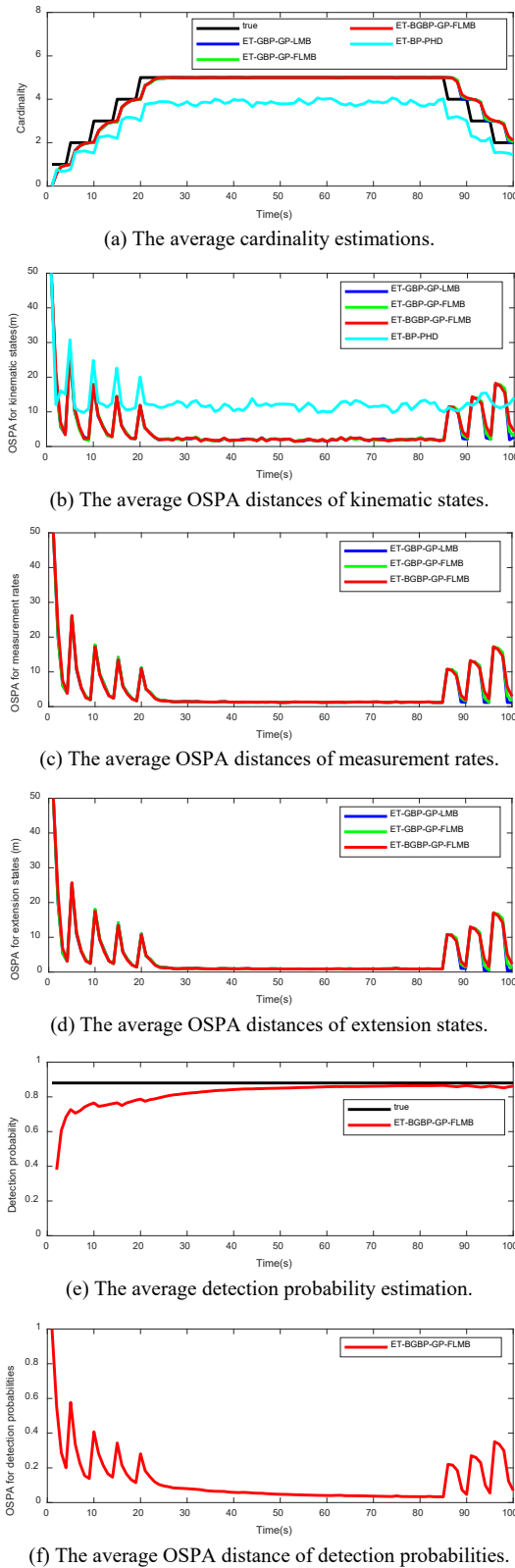
(a) The average cardinality estimations.

(b) The average OSPA distances of kinematic states.

(c) The average OSPA distances of measurement rates.

(d) The average OSPA distances of extension states.

(e) The average detection probability estimation.

(f) The average OSPA distance of detection probabilities.

Fig. 4. The average results of 100 Monte Carlo simulations.

Filter	Run time (s)
ET-GBP-GP-LMB	101.1277
ET-GBP-GP-FLMB	38.6171
ET-BGBP-GP-FLMB	44.7009
ET-BP-PHD	20.9468

Tab. 2. The average running time statistics.

ity estimation. Due to the low detection probability in this simulation, the possibility of continuous missed detection of each target is increased, so the three filter cardinality estimation delays are aggravated. It can be seen from Fig. 4(e) that, when the detection probability is low, the proposed ET-BGBP-GP-FLMB filter can still obtain a relatively accurate estimation of detection probability. It can be seen from Tab. 2 that the running time of the ET-GBP-GP-FLMB filter is significantly shorter than that of the ET-GBP-GP-LMB filter, and the ET-BGBP-GP-FLMB filter is similar to the ET-GBP-GP-FLMB filter.

5.2 Simulation 2

To further verify the tracking performance of the proposed filter, a nonlinear scenario is set up in this simulation. Similarly, considering the huge computational burden of the SMC implementation, this simulation only compares the ET-GBP-GP-LMB, ET-GBP-GP-FLMB, ET-BGBP-GP-FLMB and ET-BP-PHD filters. The surveillance area of this simulation is $[0, \pi]\,\text{(rad)} \times [0, 2000]\,\text{(m)}$, and the monitoring duration is 1–100 s. A total of four targets with different shapes appeared successively in the surveillance area, and their real shapes are shown in Fig. 5(a). In this simulation, the extension states are all set to irregular shapes. The motion of each target is still modeled as a CV model with a process noise standard deviation $\sigma_{\mathbf{w}_{k-1}^{\text{K}}} = 10\,\text{m/s}^2$. The detection probability and the average number of clutter are set to 0.88 and 10, respectively. The sensor is at the origin, the measurement sources are distributed on the target contour. The relationship between measurement source and measurement is as follows

$$\mathbf{z}_k = h(\mathbf{x}_{s,k}) + \mathbf{v}_k, \tag{96}$$

$$h(\mathbf{x}_{s,k}) = \left(\arctan(\mathbf{x}_{s,y,k} / \mathbf{x}_{s,x,k}), \sqrt{\mathbf{x}_{s,x,k}^2 + \mathbf{x}_{s,y,k}^2} \right)^{\text{T}}, \tag{97}$$

$$\mathbf{x}_{s,k} = \mathbf{x}_k^c + \mathbf{p}_k^{\text{E}}(\theta_k^{\text{E}}) f_k^{\text{E}}(\theta_k^{\text{E}}) \tag{98}$$

where $\mathbf{x}_{s,k} = (\mathbf{x}_{s,x,k}, \mathbf{x}_{s,y,k})^{\text{T}}$ is the measurement source, θ_k^{E} obeys a uniform distribution over $[0, 2\pi]$. The measurement noise obeys a Gaussian distribution with zero mean, and its standard deviations in the polar angle and polar radial directions are $\sigma_\theta = 0.01°$ and $\sigma_r = 0.1\,\text{m}$, respectively. The clutter is evenly distributed in the surveillance area. The survival time of the first target is 1–80 s, the survival time of the second target is 5–90 s, the survival time of the third target is 10–100 s, and the survival time of the fourth target is 15–100 s. Considering that the shape of each target is irregular in this simulation, the extension state of each target is set to 100 dimensions, i.e., $N^{\text{E}} = 100$. In addition, for the ET-GBP-GP-LMB, ET-GBP-GP-FLMB and ET-BGBP-GP-FLMB filters, the requested number of hypothesis components for GLMB update is set to 100. The settings of other simulation parameters are the same as those in Sec. 5.1. The single tracking result of the ET-BGBP-GP-FLMB filter is shown in Fig. 5(b). The average results of 100 Monte Carlo simulations are shown in Fig. 6 and Tab. 3.

In Fig. 5(b), the meanings of black solid lines, circles, triangles and different colors are the same as those in Fig. 2. It can be seen that the proposed ET-BGBP-GP-FLMB filter can still track each extended target well and maintain their tracks, although the detection condition is poor in this simulation. It can be seen from Fig. 6 that the
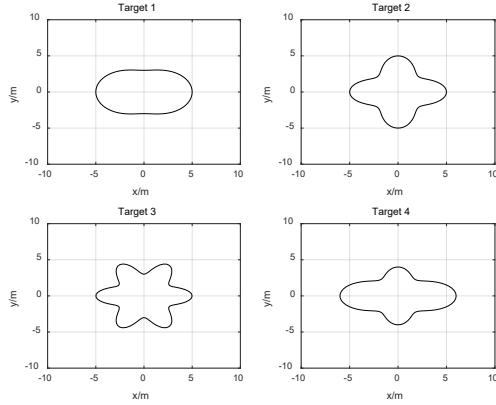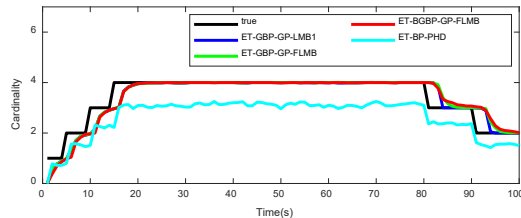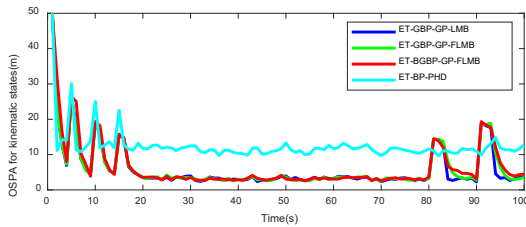

(a) The real shapes.
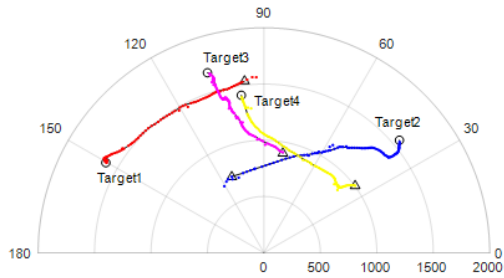
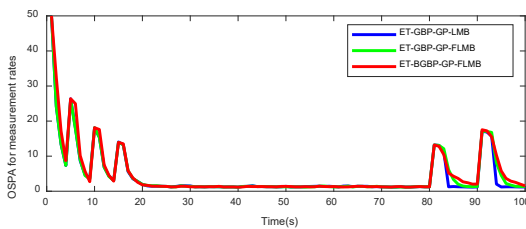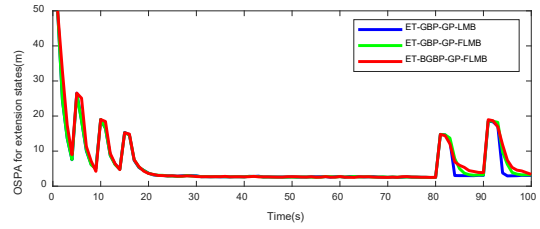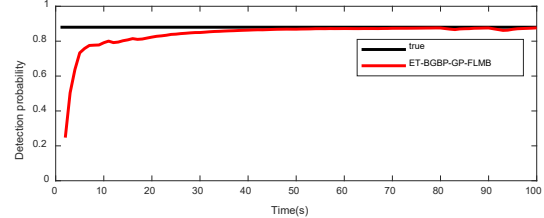(b) The single tracking result of the ET-BGBP-GP-FLMB filter.

Fig. 5. The real shapes and single tracking result.

(a) The average cardinality estimations.

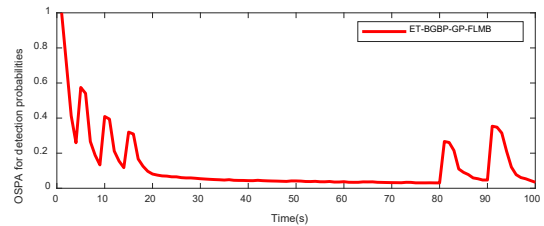(b) The average OSPA distances of kinematic states.

(c) The average OSPA distances of measurement rates.

(d) The average OSPA distances of extension states.

(e) The average detection probability estimation.

(f) The average OSPA distance of detection probabilities.

Fig. 6. The average results of 100 Monte Carlo simulations.

Filter	Run time (s)
ET-GBP-GP-LMB	136.4984
ET-GBP-GP-FLMB	43.0297
ET-BGBP-GP-FLMB	45.3201
ET-BP-PHD	16.2161

Tab. 3. The average running time statistics.

ET-GBP-GP-LMB, ET-GBP-GP-FLMB and ET-BGBP-GP-FLMB filters have similar estimation performance, which is significantly better than the ET-BP-PHD filter, and their cardinality estimations are delayed at target birth and death moments. In terms of running time, the same conclusion can be drawn from Tab. 3 as Tab. 2. See Sec. 5.1 for a theoretical analysis of these phenomena.

6. Conclusions

This paper proposes a new ET-FLMB filter, and its BGBP-GP implementation is given. Compared with the ET-LMB filter, the proposed ET-FLMB filter effectively reduces the number of hypothesis components and computational complexity. Compared with the traditional SMC implementation, the box particle implementation effectively reduces the number of particles and computational burden. In addition, the proposed filter can recursively estimate the unknown detection probability, measurement rate and extension state with arbitrary star-convex shape of each extended target, effectively expanding its application scope. In practical applications, the proposed filter can be embedded into a DSP signal processing board and connected to the actual tracking system to achieve extended

target tracking. What's more, based on the proposed filter, we can also consider the classification and recognition of targets according to their different shapes in future work.

Acknowledgments

References

[1] SCHIKORA, M., GNING, A., MIHAYLOVA, L., et al. Box-particle probability hypothesis density filtering, *IEEE Transactions on Aerospace and Electronic Systems,* 2014, vol. 50, no. 3, p. 1660–1672. DOI: 10.1109/TAES.2014.120238

[2] ZHAO, X., SONG, L. Box-particle cardinality balanced multi-target multi-Bernoulli filter. *Radioengineering,* 2014, vol. 23, no. 2, p. 609–617. ISSN: 1210-2512

[3] REUTER, S., VO, B. T., VO, B. N., et al. The labeled multi-Bernoulli filter. *IEEE Transactions on Signal Processing,* 2014, vol. 62, no. 12, p. 3246–3260. DOI: 10.1109/TSP.2014.2323064

[4] VO, B. N., VO, B. T., HOANG, H. G. An efficient implementation of the generalized labeled multi-Bernoulli filter. *IEEE Transactions on Signal Processing,* 2017, vol. 65, no. 8, p. 1975–1987. DOI: 10.1109/TSP.2016.2641392

[5] MAHLER, R. PHD filters for nonstandard targets, I: Extended targets. In *Proceedings of the 12th International Conference on Information Fusion.* Seattle (WA, USA), 2009, p. 915–921. ISBN: 978-0-9824-4380-4

[6] ORGUNER, U., LUNDQUIST, C., GRANSTRÖM, K. Extended target tracking with a cardinalized probability hypothesis density filter. In *Proceedings of the 14th International Conference on Information Fusion.* Chicago (IL, USA), 2011, p. 1–8.

[7] ZHANG, G., LIAN, F., HAN, C. CBMeMBer filters for nonstandard targets, I: Extended targets. In *Proceedings of the 17th International Conference on Information Fusion.* Salamanca (Spain), 2014, p. 1–6. ISBN: 978-8-4901-2355-3

[8] BEARD, M., REUTER, S., GRANSTRÖM, K., et al. Multiple extended target tracking with labelled random finite sets. *IEEE Transactions on Signal Processing,* 2016, vol. 64, no. 7, p. 1638–1653. DOI: 10.1109/TSP.2015.2505683

[9] GRANSTRÖM, K., FATEMI, M., SVENSSON, L. Poisson multi-Bernoulli mixture conjugate prior for multiple extended target filtering. *IEEE Transactions on Aerospace and Electronic Systems,* 2020, vol. 56, no. 1, p. 208–225. DOI: 10.1109/TAES.2019.2920220

[10] GRANSTRÖM, K., LUNDQUIST, C., ORGUNER, U. Extended target tracking using a Gaussian-Mixture PHD filter. *IEEE Transactions on Aerospace and Electronic Systems,* 2012, vol. 48, no. 4, p. 3268–3286. DOI: 10.1109/TAES.2012.6324703

[11] ZHANG, G., LIAN, F., HAN, C., et al. A Gaussian mixture extended-target multi-Bernoulli filter (in Chinese). *Journal of Xi'an Jiaotong University,* 2014, vol. 48, no. 10, p. 9–14. DOI: 10.7652/xjtuxb201410002

[12] LI, Y., XIAO, H., SONG, Z., et al. A new multiple extended target tracking algorithm using PHD filter. *Signal Processing,* 2013, vol. 93, no. 12, p. 3578–3588. DOI: 10.1016/j.sigpro.2013.05.011

[13] MA, D., LIAN, F., LIU, J. Sequential Monte Carlo implementation of cardinality balanced multi-target multi-Bernoulli filter for extended target tracking. *IET Radar, Sonar and Navigation,* 2016, vol. 10, no. 2, p. 272–277. DOI: 10.1049/iet-rsn.2015.0081

[14] LUNDQUIST, C., GRANSTRÖM, K., ORGUNER, U. An extended target CPHD filter and a gamma Gaussian inverse Wishart implementation. *IEEE Journal of Selected Topics in Signal Processing,* 2013, vol. 7, no. 3, p. 472–483. DOI: 10.1109/JSTSP.2013.2245632

[15] ZHANG, Y., JI, H., HU, Q. A fast ellipse extended target PHD filter using box-particle implementation. *Mechanical Systems and Signal Processing,* 2018, vol. 99, p. 57–72. DOI: 10.1016/j.ymssp.2017.05.044

[16] ZHANG, Y., JI, H., GAO, X., et al. An ellipse extended target CBMeMBer filter using gamma and box-particle implementation. *Signal Processing,* 2018, vol. 149, p. 88–102. DOI: 10.1016/j.sigpro.2018.03.002

[17] CHENG, X., JI, H., ZHANG, Y. Multiple extended target tracking based on gamma box particle and labeled random finite sets. *Digital Signal Processing,* 2023, vol. 134, p. 1–27. DOI: 10.1016/j.dsp.2022.103902

[18] LIANG, Z., LIU, F., LI, L., et al. Improved generalized labeled multi-Bernoulli filter for non-ellipsoidal extended targets or group targets tracking based on random sub-matrices. *Digital Signal Processing,* 2020, vol. 99, p. 1–25. DOI: 10.1016/j.dsp.2020.102669

[19] GONG, Y., CUI, C., WU, B. A GGIW-PHD filter for multiple non-ellipsoidal extended targets tracking with varying number of sub-objects. *IEEE Access,* 2021, vol. 9, p. 64719–64731. DOI: 10.1109/access.2021.3075941

[20] WANG, L., ZHAN, R., LIU, S., et al. Joint tracking and classification of multiple extended targets via the PHD filter and star-convex RHM. *Digital Signal Processing,* 2021, vol. 111, p. 1–24. DOI: 10.1016/j.dsp.2020.102961

[21] LIU, Y., JI, H., ZHANG, Y. A multiple extended target generalized labeled multi-Bernoulli filter based on joint likelihood function (in Chinese). *Journal of Electronics & Information Technology,* 2022, vol. 45, no. 4, p. 1303–1312. DOI: 10.11999/JEIT220213

[22] ZHANG, Y., JI, H., HU, Q. A box-particle implementation of standard PHD filter for extended target tracking. *Information Fusion,* 2017, vol. 34, p. 55–69. DOI: 10.1016/j.inffus.2016.06.007

[23] LI, M., LIN, Z., AN, W., et al. Box-particle labeled multi-Bernoulli filter for multiple extended target tracking. *Radioengineering,* 2016, vol. 25, no. 3, p. 527–535. DOI: 10.13164/re.2016.0527

[24] WAHLSTRÖM, N., ÖZKAN, E. Extended target tracking using Gaussian processes. *IEEE Transactions on Signal Processing,* 2015, vol. 63, no. 16, p. 4165–4178. DOI: 10.1109/TSP.2015.2424194

[25] GRANSTRÖM, K., ORGUNER, U. Estimation and maintenance of measurement rates for multiple extended target tracking. In *Proceeding of the 15th International Conference on Information Fusion.* Singapore, 2012, p. 2170–2176.

[26] SCHUHMACHER, D., VO, B. T., VO, B. N. A consistent metric for performance evaluation of multi-object filters. *IEEE Transactions on Signal Processing,* 2008, vol. 86, no. 8, p. 3447–3457. DOI: 10.1109/TSP.2008.920469

About the Authors ...

Xuan CHENG was born in 1991. He is a Ph.D. degree candidate at Xidian University. His research interests include target tracking and nonlinear filtering.

Hongbing JI (corresponding author) was born in 1963. He received his Ph.D. degree from Xidian University. He is currently a Professor and doctoral supervisor of Xidian University. His research interests include intelligent information processing, target tracking and recognition, and multi-sensor information fusion.

Yongquan ZHANG was born in 1985. He received his Ph.D. degree from Xidian University. He is now an Associate Professor of Xidian University. His research interests include target detection and tracking, machine learning and nonlinear filtering.